

# The Role of Drifts and Radiating Species in Detached Divertor Operation at DIII-D

**A.G. McLean<sup>1</sup>**

with S.L. Allen<sup>1</sup>, T. Abrams<sup>3</sup>, J.A. Boedo<sup>5</sup>, I. Bykov<sup>5</sup>, A. Briesemeister<sup>2</sup>, J. Canik<sup>2</sup>, R. Ding<sup>6</sup>, D. Elder<sup>4</sup>, D. Eldon<sup>7</sup>, M. Fenstermacher<sup>1</sup>, M. Groth<sup>8</sup>, H.Y. Guo<sup>3</sup>, J. Guterl<sup>3</sup>, D.N. Hill<sup>3</sup>, A. Jarvinen<sup>1</sup>, E. Kolemen<sup>7</sup>, C. Lasnier<sup>1</sup>, A.W. Leonard<sup>3</sup>, M. Makowski<sup>1</sup>, B. Meyer<sup>1</sup>, A.L. Moser<sup>3</sup>, T.H. Osborne<sup>3</sup>, T.W. Petrie<sup>3</sup>, G.D. Porter<sup>1</sup>, T. Rognlien<sup>1</sup>, D. Rudakov<sup>5</sup>, C. Samuell<sup>1</sup>, C. Sang<sup>6</sup>, P.C. Stangeby<sup>4</sup>, D. Thomas<sup>3</sup>, E. Unterberg<sup>2</sup>, H. Wang<sup>2</sup>, J. Watkins<sup>9</sup>

<sup>1</sup>LLNL

<sup>2</sup>ORNL

<sup>3</sup>GA

<sup>4</sup>University of Toronto

<sup>5</sup>UCSD

<sup>6</sup>ASIPP

<sup>7</sup>PPPL

<sup>8</sup>Aalto University

<sup>9</sup>SNL

Presented at the  
**26<sup>th</sup> International Atomic Energy Agency  
Fusion Energy Conference**  
Kyoto, Japan

**October 17–22, 2016**

**Divertor & SOL Physics 1, 19 Oct. 10:45-11:05 AM**



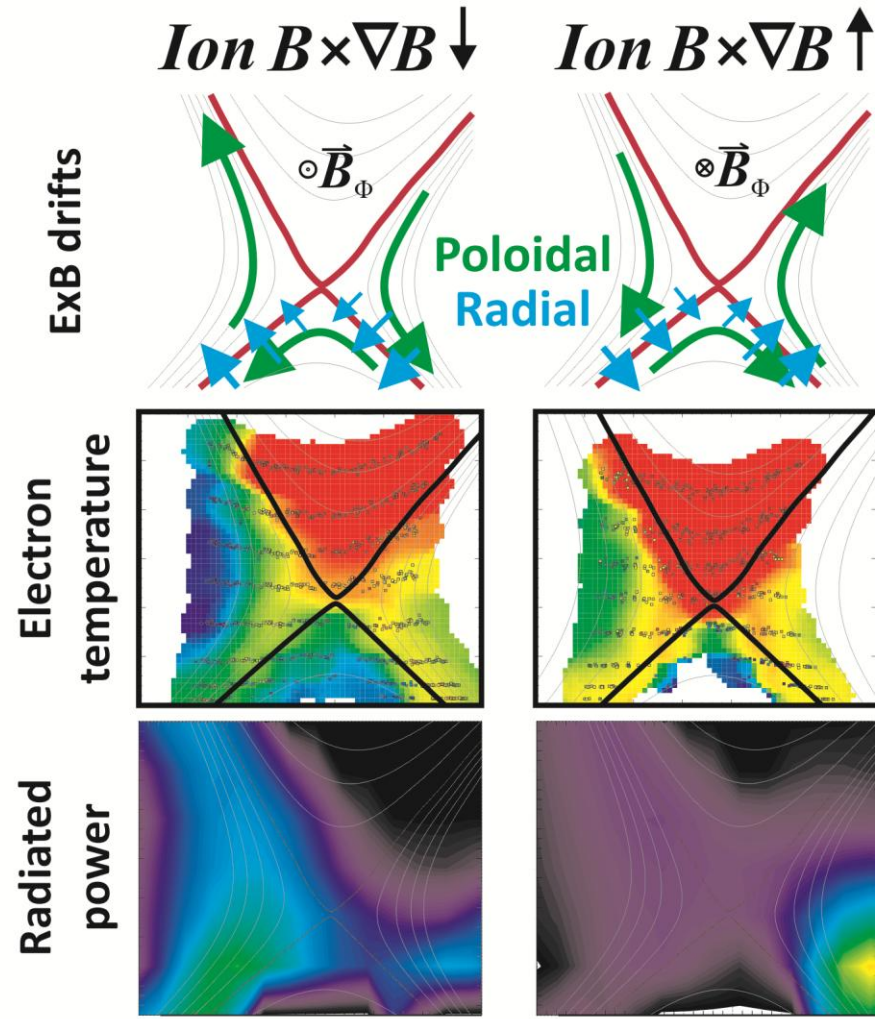
McLean/IAEA FEC/October 2016

This work was performed under the auspices of the U.S. Department of Energy by Lawrence Livermore National Laboratory under Contract DEAC52-07NA27344, and under Contracts DE-FC02-04ER54698, DEFG02-07ER54917, DE-FG02-05ER54809. LLNL-PRES-704559



# Prediction and Control of Target Heat Load is Critical for Future Devices

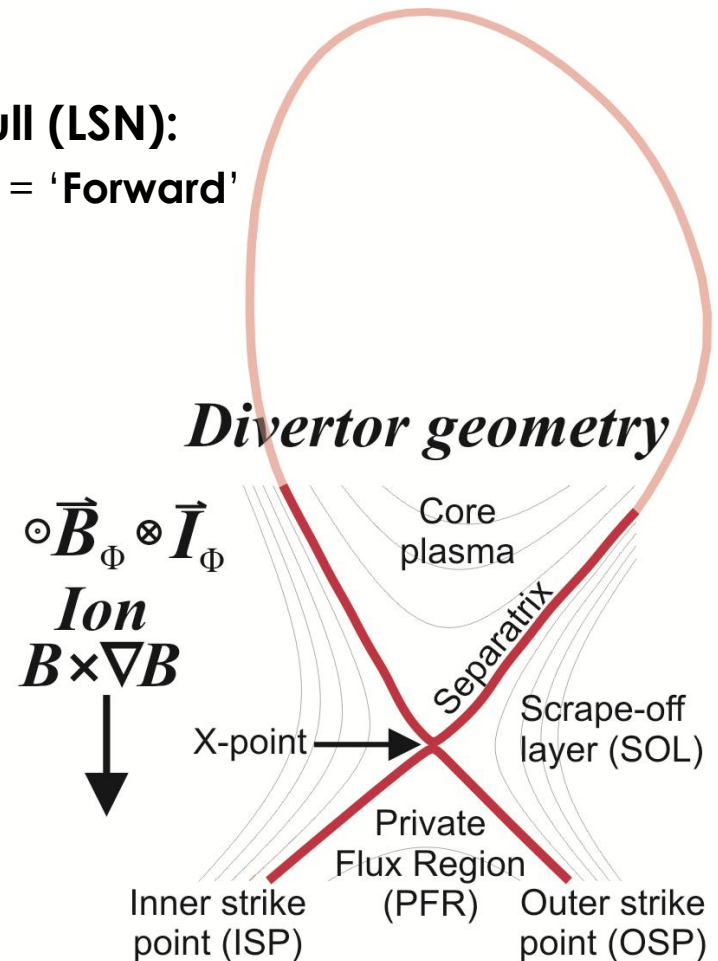
- **Inner/outer target asymmetries**
  - Roles of  $\mathbf{E} \times \mathbf{B}$  drift components
  - Result: Qualitative agreement between experiment and 2D fluid modeling with drifts
- **Detachment onset**
  - 2D measurements with Divertor Thomson scattering (DTS)
  - Result: Rapid transition to a cold outer target with ion  $B \times \nabla B \downarrow$
- **Radiated power**
  - Universal shortfall when modeling compared to experiment, multiple codes and wall materials
  - Result: No shortfall in He plasma using divertor conditions as input





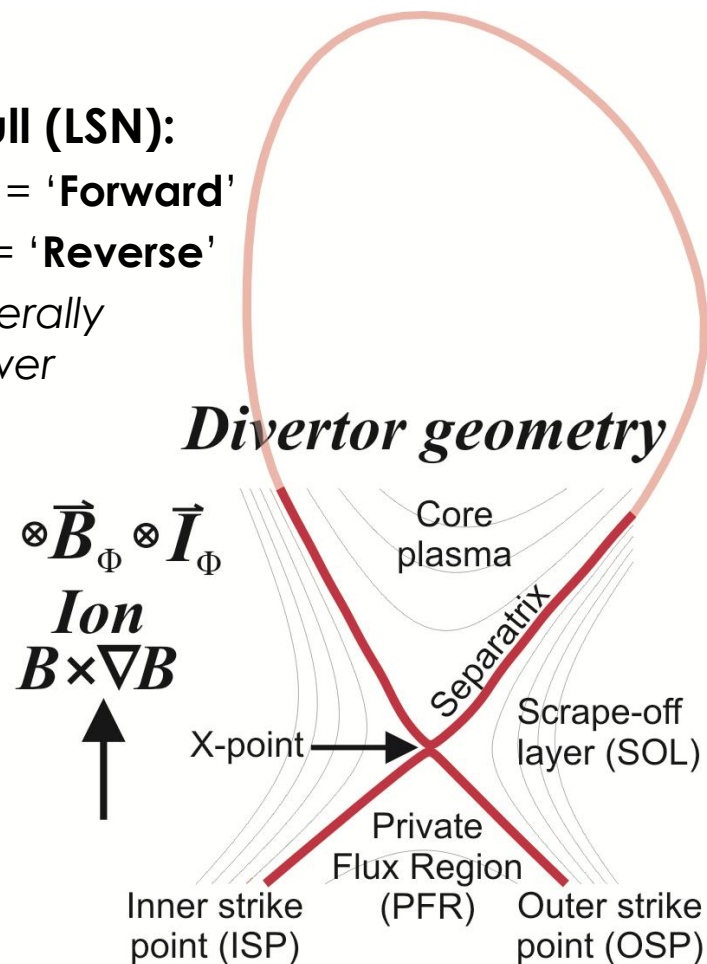
# Reversing the Toroidal B Field is Carried Out to Probe the Impact of $E \times B$ Drifts in the Divertor

- **Toroidal field convention – lower single null (LSN):**
  - Ion  $B \times \nabla B$  direction **down** (into the divertor) = ‘**Forward**’



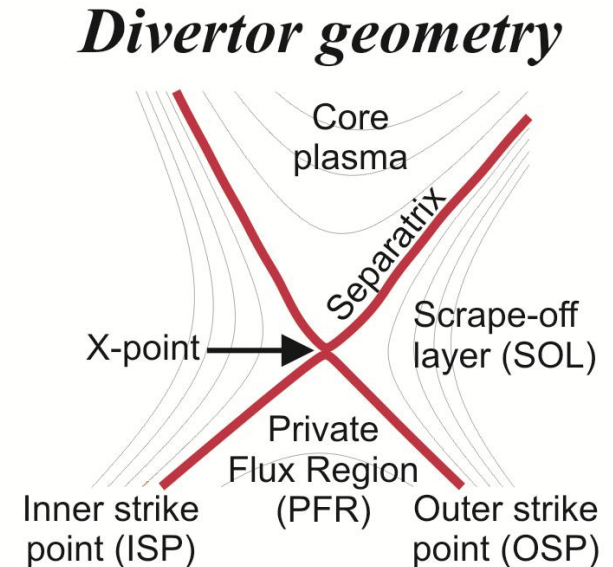
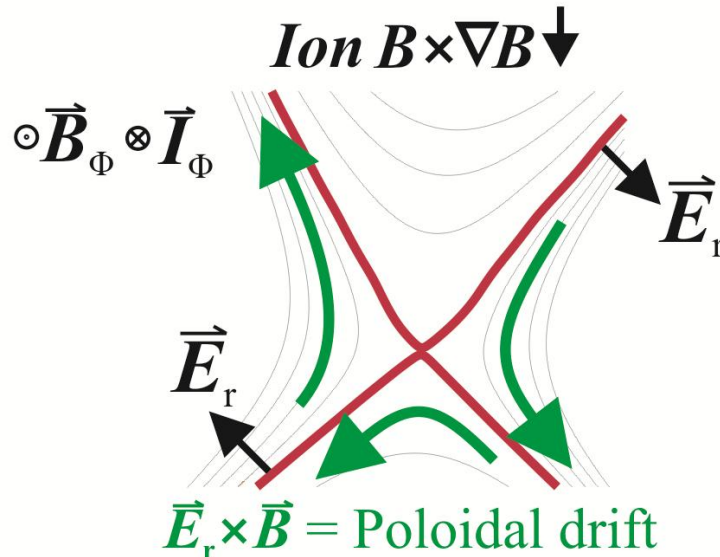
# Reversing the Toroidal B Field is Carried Out to Probe the Impact of $E \times B$ Drifts in the Divertor

- **Toroidal field convention – lower single null (LSN):**
  - Ion  $B \times \nabla B$  direction **down** (into the divertor) = '**Forward**'
  - Ion  $B \times \nabla B$  direction **up** (out of the divertor) = '**Reverse**'
  - In fwd  $B_r$ , less power to enter H-mode, generally higher confinement for equal injected power
    - '**Favorable**' direction



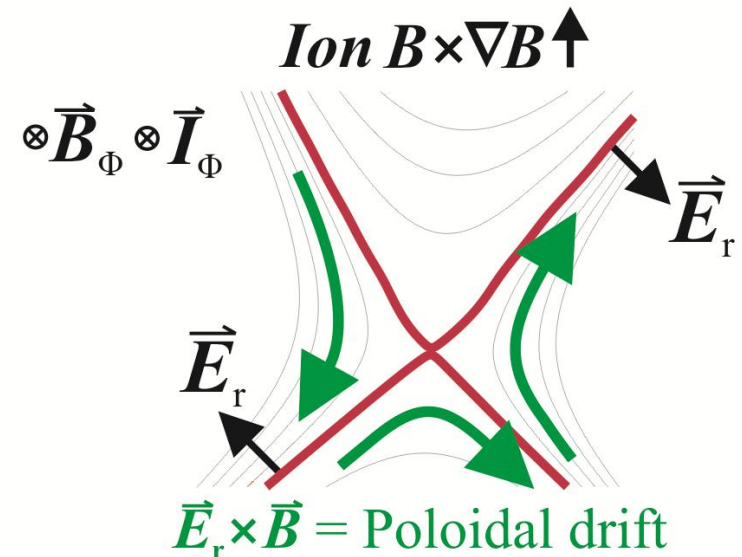
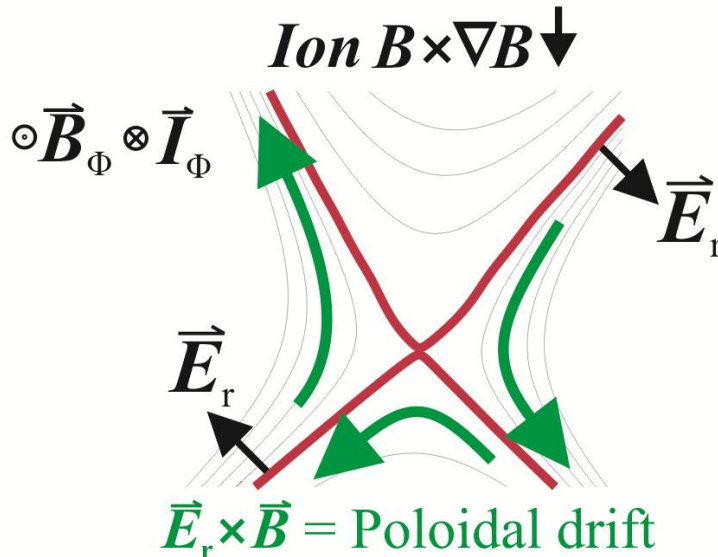
# $E \times B$ Drifts Can Be Separated Into Two Distinct Components

- **Poloidal**  $E_r \times B$  leads to flow of particles from
  - outer to inner divertor in the PFR with ion  $B \times \nabla B \downarrow$



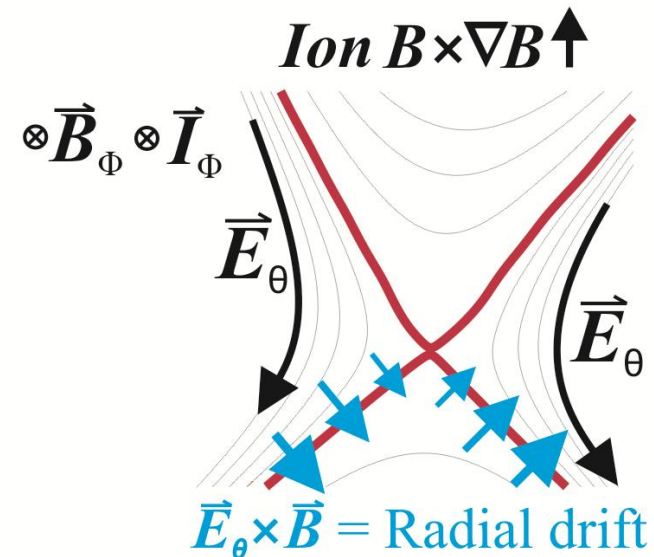
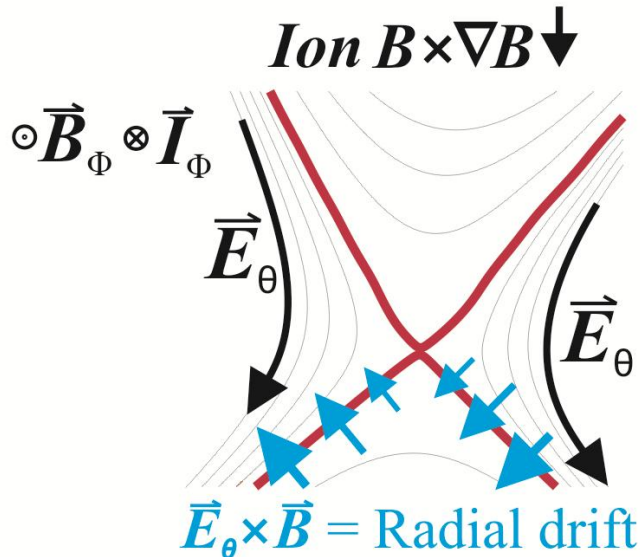
# $E \times B$ Drifts Can Be Separated Into Two Distinct Components

- **Poloidal  $E_r \times B$  leads to flow of particles from**
  - *outer to inner* divertor in the PFR with ion  $B \times \nabla B \downarrow$
  - *inner to outer* divertor in the PFR with ion  $B \times \nabla B \uparrow$



# $E \times B$ Drifts Can Be Separated Into Two Distinct Components

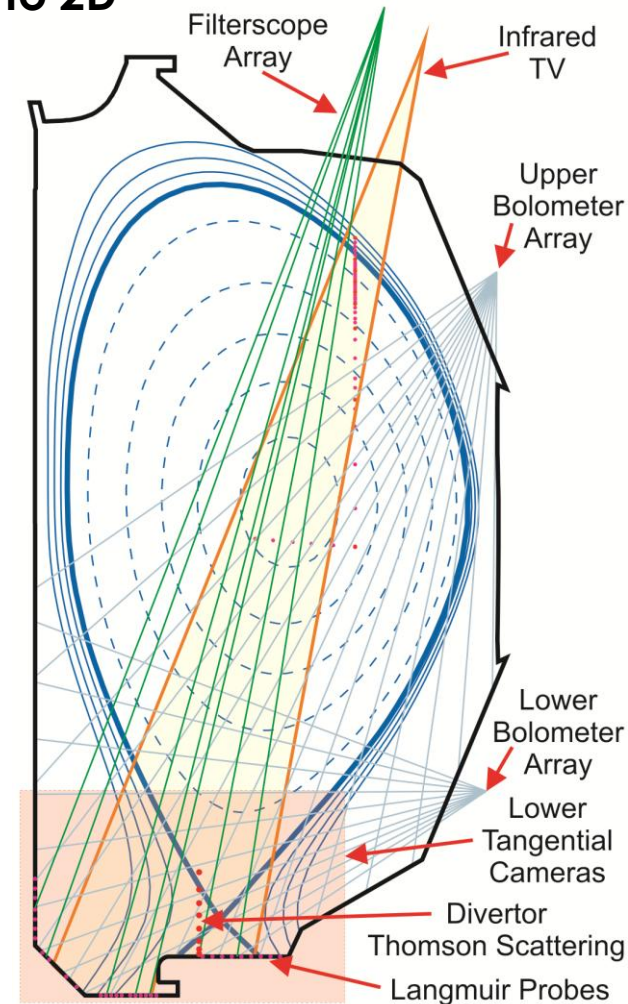
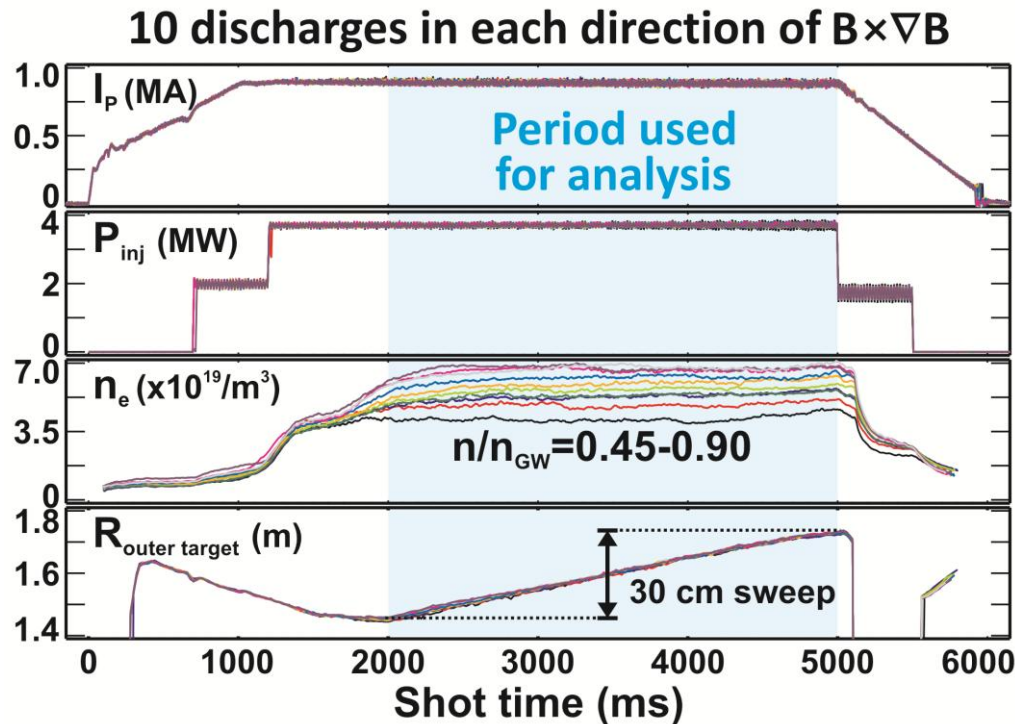
- **Poloidal  $E_r \times B$  leads to flow of particles from**
  - *outer to inner* divertor in the PFR with ion  $B \times \nabla B \downarrow$
  - *inner to outer* divertor in the PFR with ion  $B \times \nabla B \uparrow$
- **Radial  $E_\theta \times B$  carries particles**
  - into/out of the PFR from the outboard side with ion  $B \times \nabla B \downarrow$ 
    - Leads to *inward* shifts in radial profiles
  - into/out of the PFR from the inboard side with ion  $B \times \nabla B \uparrow$ 
    - Leads to *outward* shifts in radial profiles





# Well Characterized Plasmas are Used to Reveal the Impacts of Drifts

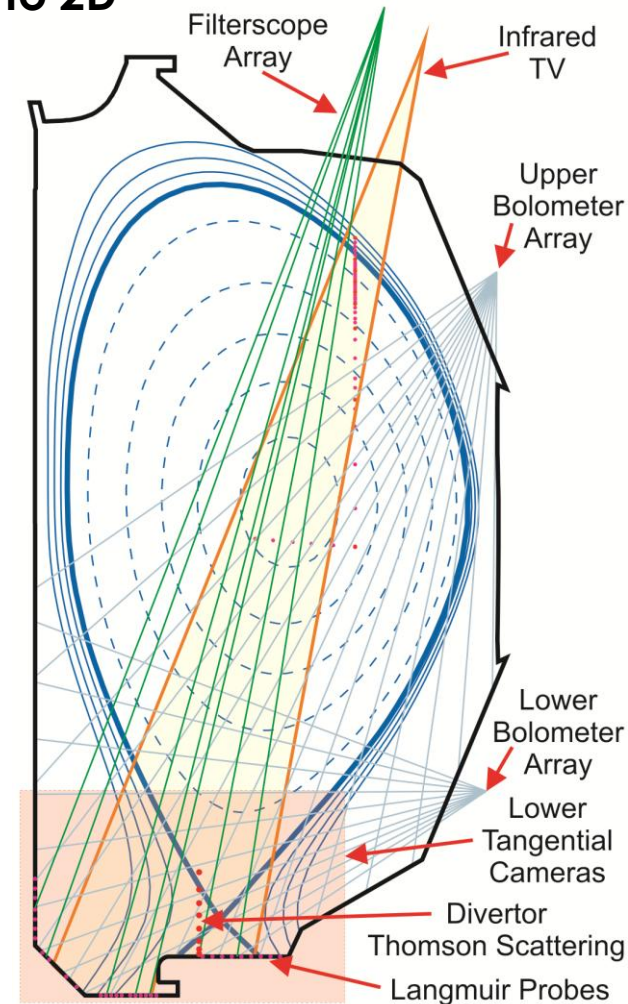
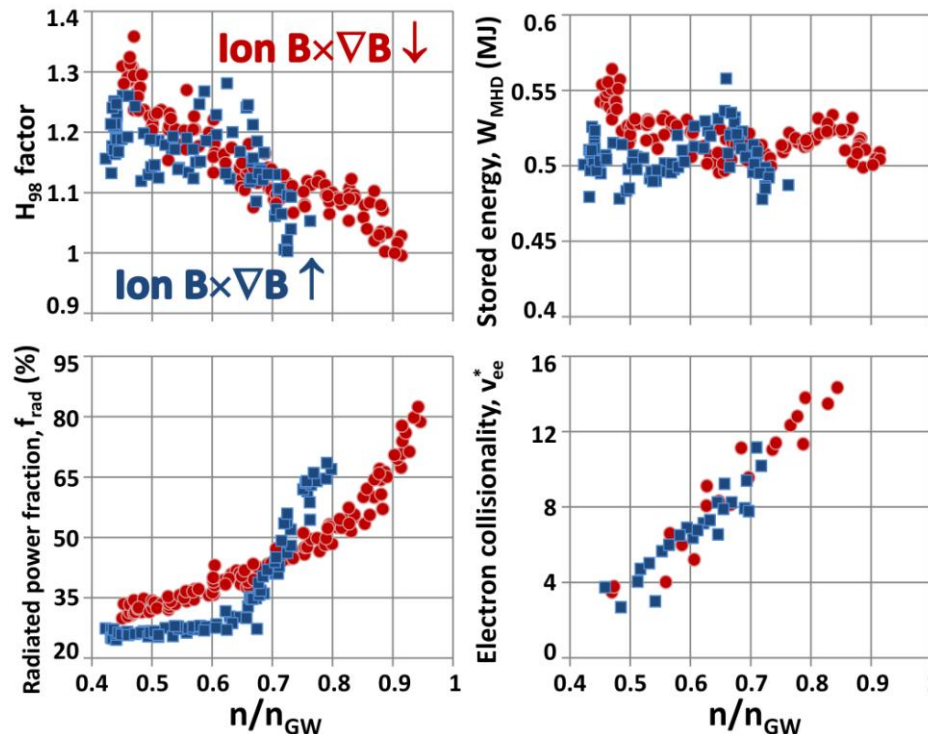
- Increasing steady density step in successive discharges
- Swept X-point across 1D diagnostic arrays to extend to 2D
- Upgraded diagnostics including 2D remapped DTS
- Inter-ELM data analyzed





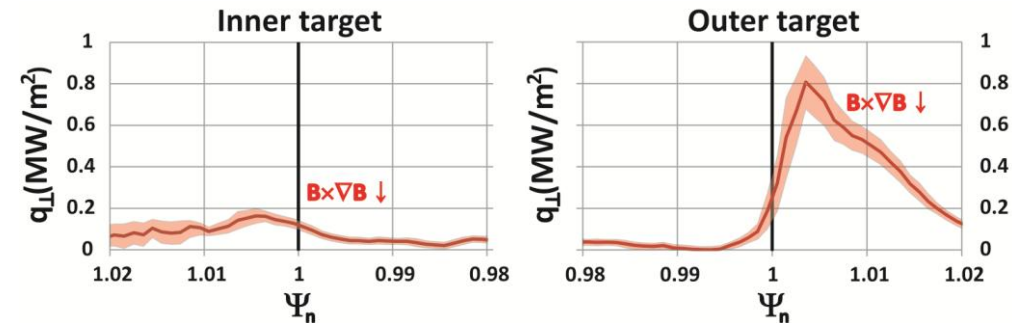
# Well Characterized Plasmas With Good Performance are Used to Reveal the Impacts of Drifts

- Increasing steady density step in successive discharges
- Swept X-point across 1D diagnostic arrays to extend to 2D
- Upgraded diagnostics including 2D remapped DTS
- Inter-ELM data analyzed
- H-mode with  $H_{98} \geq 1.0$  maintained at all  $n/n_{GW}$



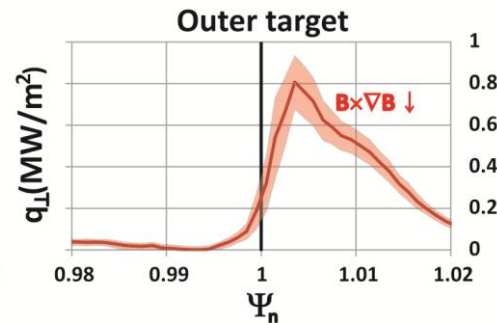
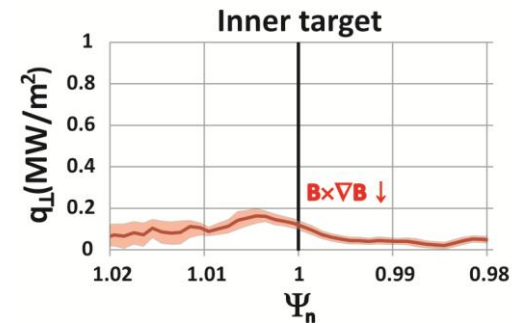
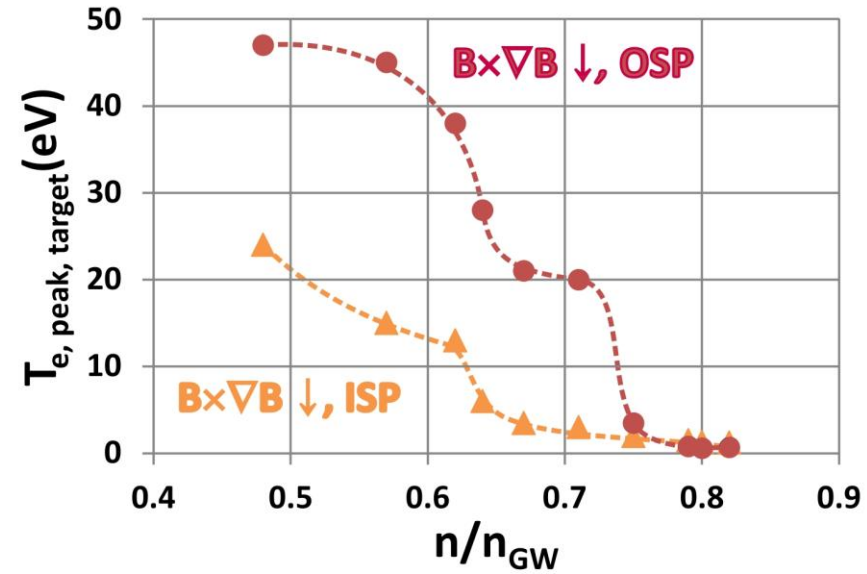
# Target Temperature Asymmetry With $B \times \nabla B \downarrow$ is Reduced For $B \times \nabla B \uparrow$ and Decreases with Increasing Density

- Target heat flux higher at outer target with  $B \times \nabla B \downarrow$



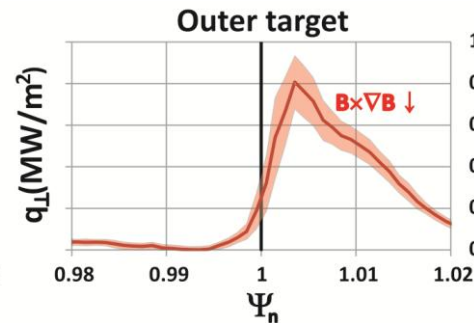
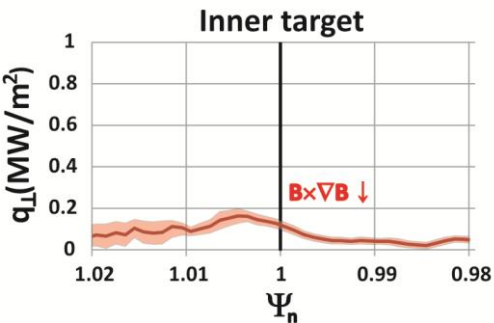
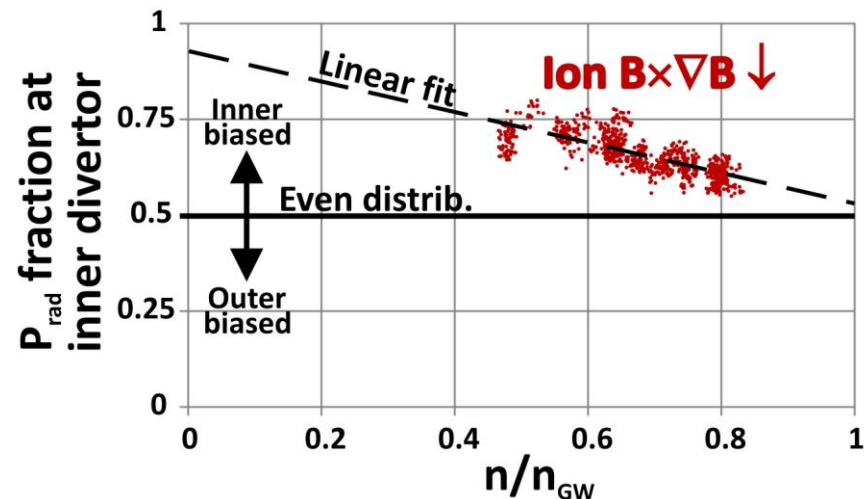
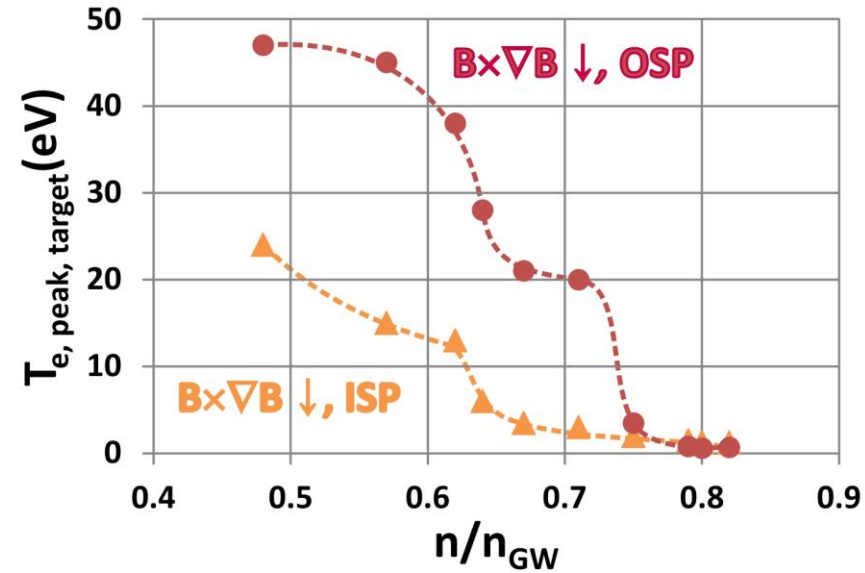
# Target Temperature Asymmetry With $B \times \nabla B \downarrow$ is Reduced For $B \times \nabla B \uparrow$ and Decreases with Increasing Density

- Target heat flux higher at outer target with  $B \times \nabla B \downarrow$
- Target  $T_e$  higher at the OSP with  $B \times \nabla B \downarrow$



# Target Temperature Asymmetry With $B \times \nabla B \downarrow$ is Reduced For $B \times \nabla B \uparrow$ and Decreases with Increasing Density

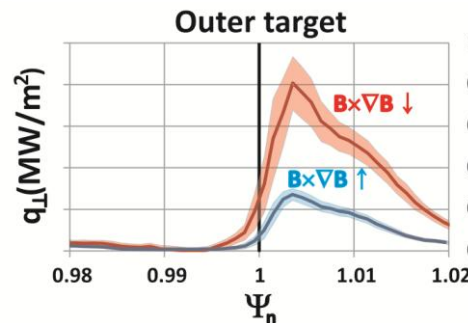
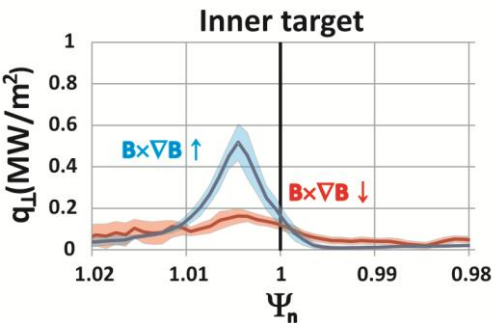
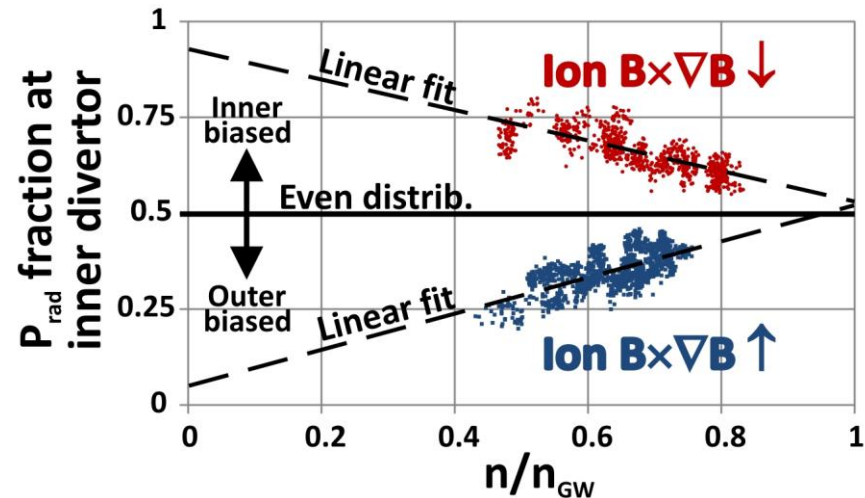
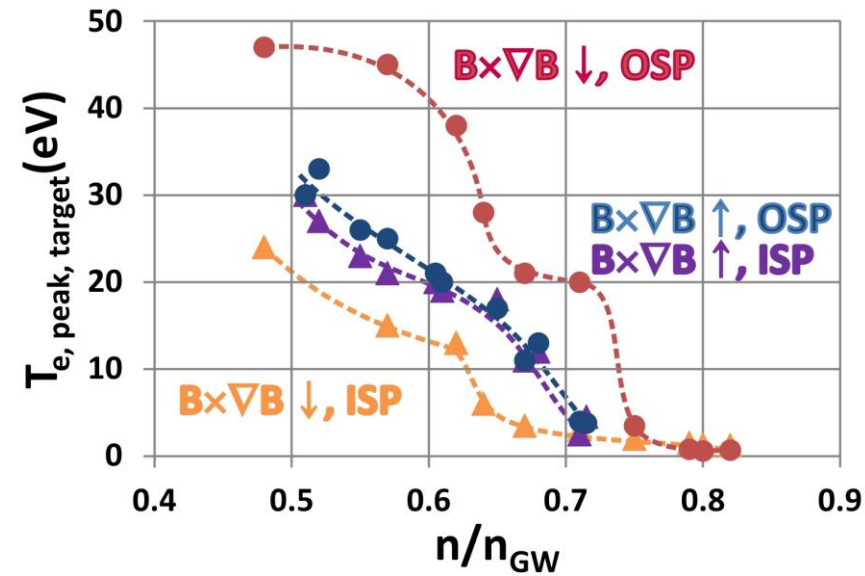
- Target heat flux higher at outer target with  $B \times \nabla B \downarrow$
- Target  $T_e$  higher at the OSP with  $B \times \nabla B \downarrow$
- Integrated radiation biased to the inner divertor with  $B \times \nabla B \downarrow$
- Targets show largest asymmetry at lowest density with  $B \times \nabla B \downarrow$





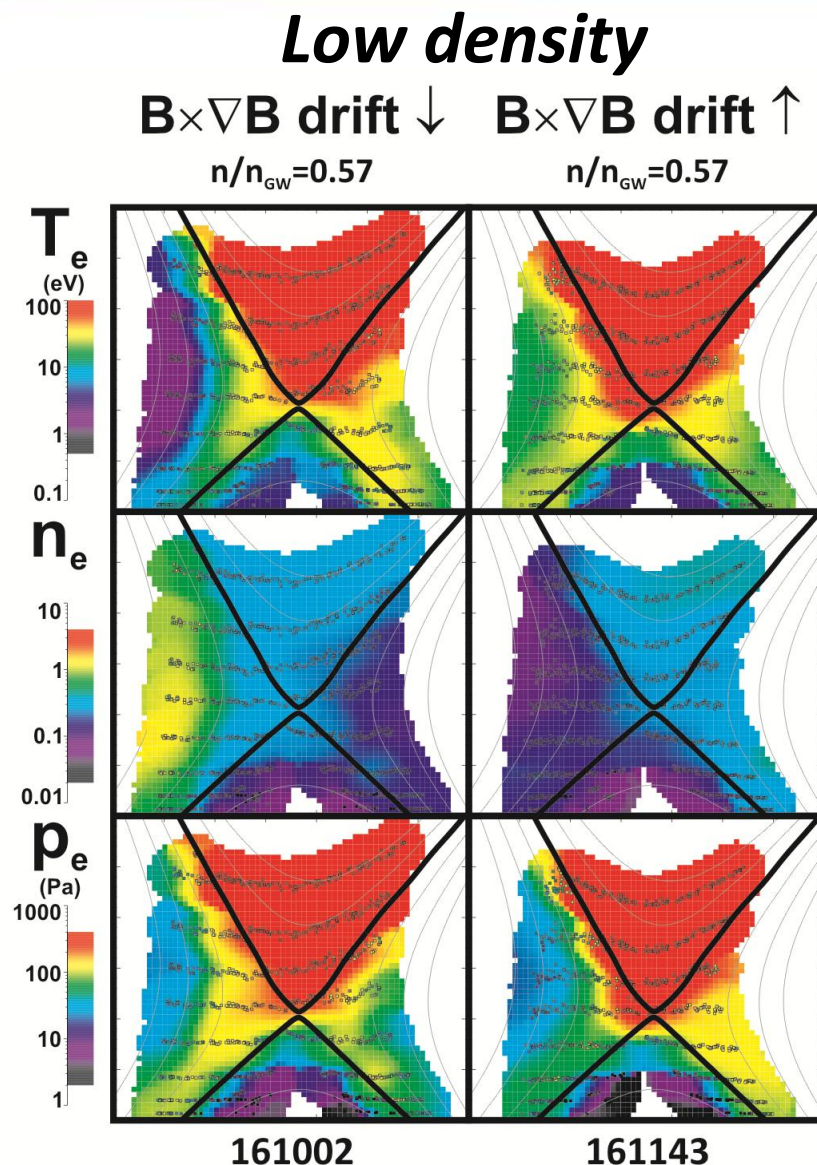
# Target Temperature Asymmetry With $B \times \nabla B \downarrow$ is Reduced For $B \times \nabla B \uparrow$ and Decreases with Increasing Density

- Target heat flux higher at outer target with  $B \times \nabla B \downarrow$ 
  - Nearly symmetric with  $B \times \nabla B \uparrow$
- Target  $T_e$  higher at the OSP with  $B \times \nabla B \downarrow$ 
  - Symmetric with  $B \times \nabla B \uparrow$
- Integrated radiation biased to the inner divertor with  $B \times \nabla B \downarrow$ 
  - In contrast, mirrored with  $B \times \nabla B \uparrow$
- Targets show largest asymmetry at lowest density with  $B \times \nabla B \downarrow$



# At Low Densities, Drifts are Large and Drive Asymmetries Throughout the Divertor Region

- **Divertor Thomson Scattering (DTS) unique to DIII-D, capable of measurements of  $0.5 < T_e < 5 \text{ keV}$ ,  $1 \times 10^{18} < n_e < 1 \times 10^{21} / \text{m}^3$** 
  - 4 MW H-mode, inter-ELM analysis only
- **Asymmetries in plasma parameters evident with  $B \times \nabla B \downarrow$ , abated asymmetry in  $B \times \nabla B \uparrow$**
- **Extraordinarily high density throughout inboard SOL region with  $B \times \nabla B \downarrow$** 
  - Confirms measurements made via Stark Broadening at ASDEX (S. Potzel PSI2014)
  - Radial density gradient reversed for  $B \times \nabla B \uparrow$
- **Pressure higher at the target towards which the poloidal drift in the PFR is directed**
  - As predicted based on particle conservation and poloidal momentum balance (A. Chankin PPCF2015)



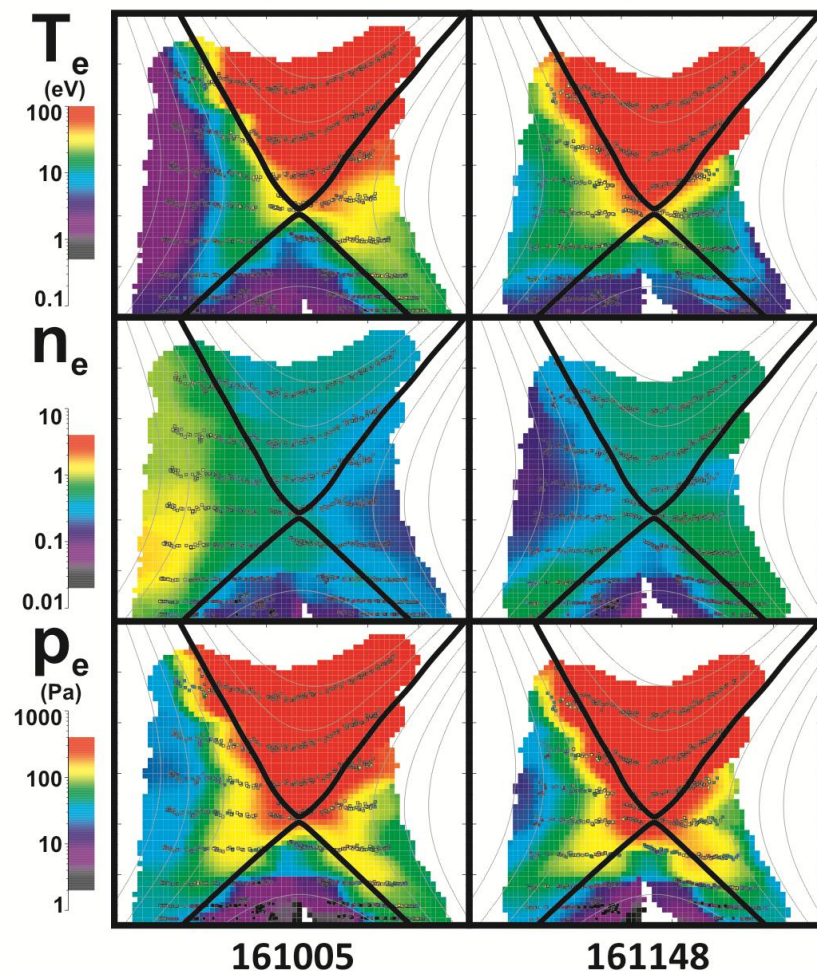
# At Medium Densities, Drifts Weaken But Their Impact Remains Observable Upstream of the Targets

- Divertor Thomson Scattering (DTS) unique to DIII-D, capable of measurements of  $0.5 < T_e < 5 \text{ keV}$ ,  $1 \times 10^{18} < n_e < 1 \times 10^{21} / \text{m}^3$ 
  - 4 MW H-mode, inter-ELM analysis only
- **Asymmetries in plasma parameters still evident with  $B \times \nabla B \downarrow$ , abated asymmetry in  $B \times \nabla B \uparrow$**
- **Transition to detachment at higher density shown to minimize the role of drifts at the targets, but not upstream in the legs**

## Medium density

$B \times \nabla B$  drift ↓  
 $n/n_{\text{GW}}=0.67$

$B \times \nabla B$  drift ↑  
 $n/n_{\text{GW}}=0.67$



161005

161148

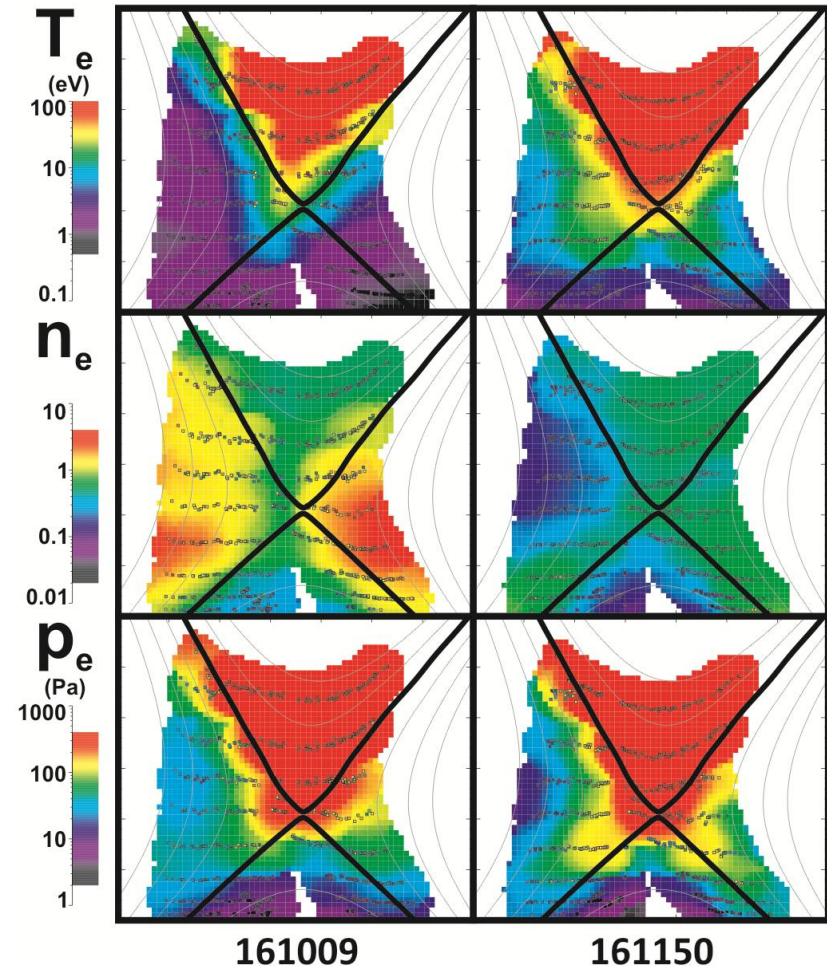


# At the Highest Densities, Impact of Drifts and Asymmetries are Minimal at the Targets

- Divertor Thomson Scattering (DTS) unique to DIII-D, capable of measurements of  $0.5 < T_e < 5 \text{ keV}$ ,  $1 \times 10^{18} < n_e < 1 \times 10^{21} / \text{m}^3$ 
  - 4 MW H-mode, inter-ELM analysis only
- Plasma parameters symmetrically cold/dense at the targets for both  $B \times \nabla B \downarrow$  and  $B \times \nabla B \uparrow$
- Sudden transition to cold/detached divertor throughout outer leg region for  $B \times \nabla B \downarrow$ 
  - Smooth transition to detachment at both legs with  $B \times \nabla B \uparrow$
- Results confirm earlier theory and modeling that show  $E \times B$  creates a particle sink in the outer SOL-divertor and a particle source in the inner SOL-divertor for  $B \times \nabla B \downarrow$ 
  - A. Chankin, Plasma Phys. Cont. Fusion 57 (2015) 095002

## High density

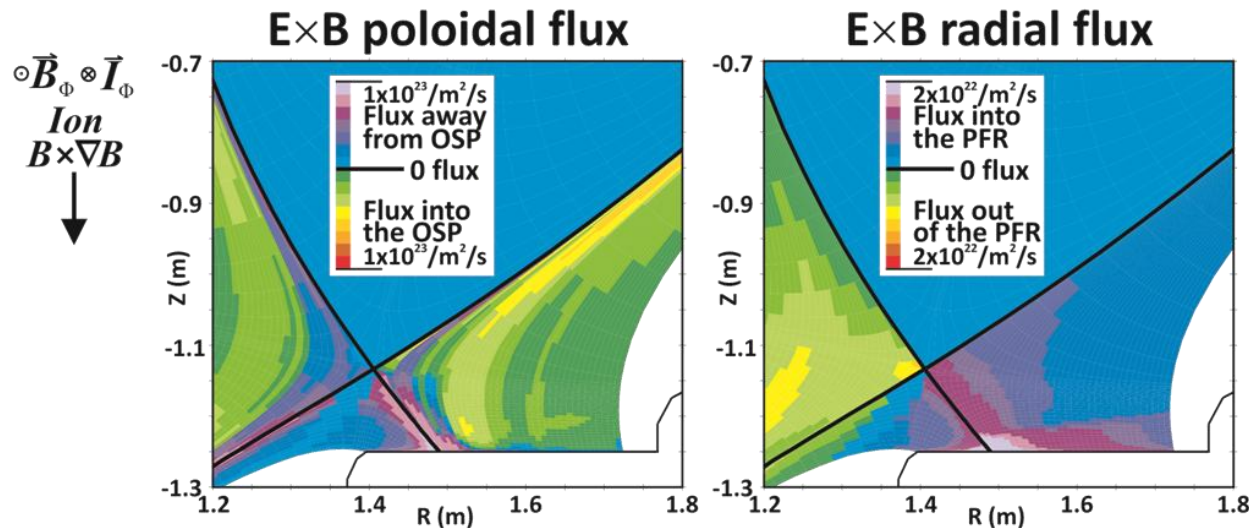
$B \times \nabla B$  drift  $\downarrow$   $n/n_{\text{GW}}=0.79$        $B \times \nabla B$  drift  $\uparrow$   $n/n_{\text{GW}}=0.72$





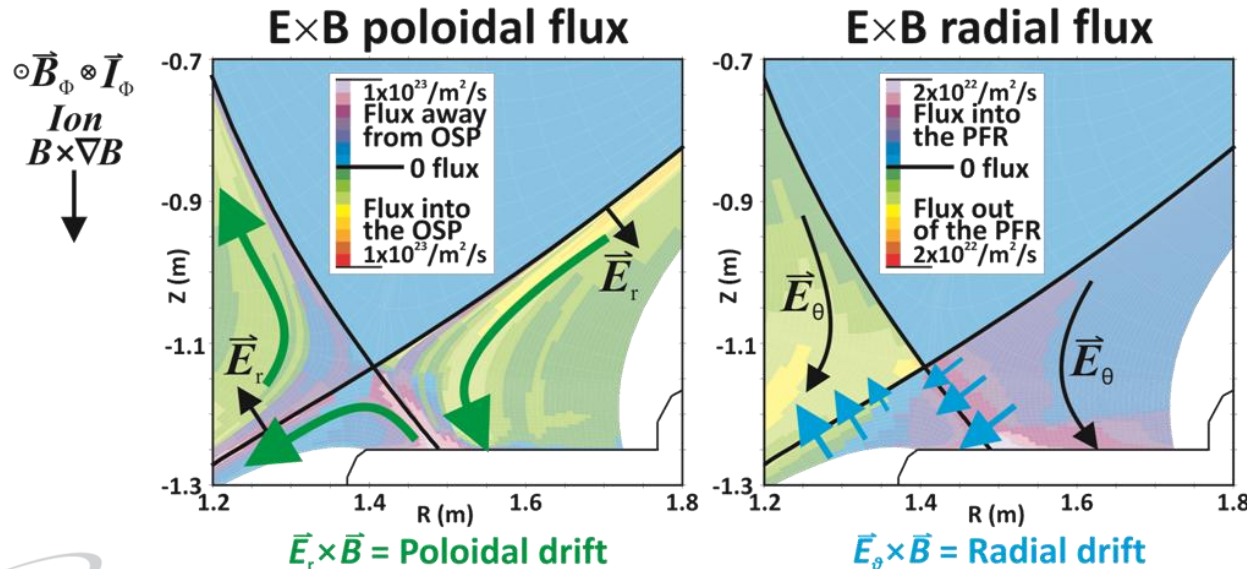
# ExB Flow Velocities and Fluxes Calculated Directly From $T_e$ and $n_e$ Measurements Confirm Strong Role of Both Radial and Poloidal Drifts

- 2D ExB drift velocities are calculated from 2D DTS measurements using Ohm's Law for the parallel electric field using OEDGE for gridding and fitting data
  - Can be done for any plasma (e.g., high power discharges)
- Spatial derivatives of  $n_e$  and  $T_e$  used to calculate  $E$ , integrated along and across flux tubes to find  $v_{\text{plasma}}$ , multiplied by local  $n$  for particle fluxes
- Integrated poloidal and radial fluxes are found to be comparable in attached conditions, as suggested by theory and modeling



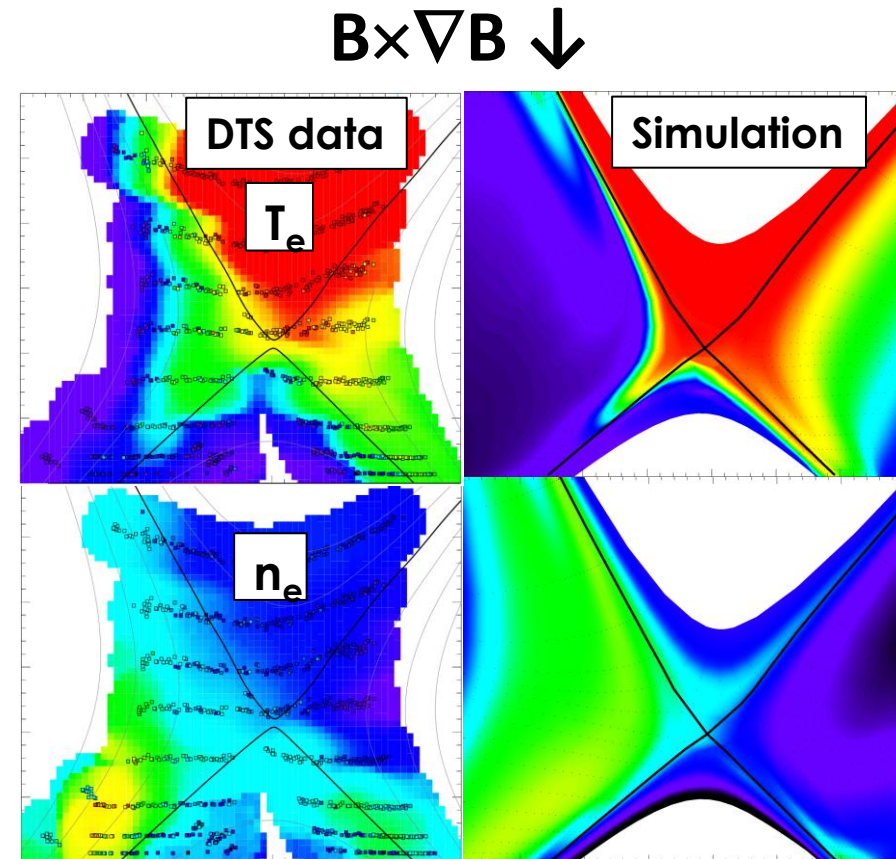
# ExB Flow Velocities and Fluxes Calculated Directly From $T_e$ and $n_e$ Measurements Confirm Strong Role of Both Radial and Poloidal Drifts

- 2D ExB drift velocities are calculated from 2D DTS measurements using Ohm's Law for the parallel electric field using OEDGE for gridding and fitting data
  - Can be done for any plasma (e.g., high power discharges)
- Spatial derivatives of  $n_e$  and  $T_e$  used to calculate  $E$ , integrated along and across flux tubes to find  $v_{\text{plasma}}$ , multiplied by local  $n$  for particle fluxes
- Integrated poloidal and radial fluxes are found to be comparable in attached conditions, as suggested by theory and modeling and fluxes match the expected drift pattern



# Modeling of DIII-D H-mode With $B \times \nabla B \downarrow$ and $\uparrow$ Using UEDGE Confirms Relative Roles of Poloidal and Radial $E \times B$ on Asymmetries

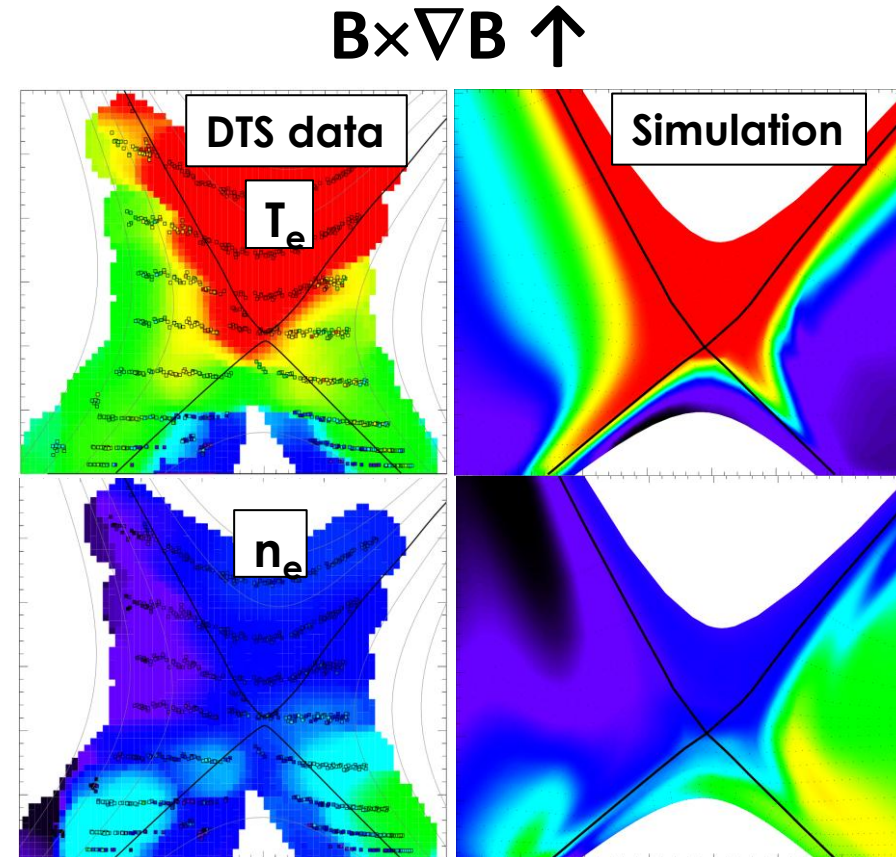
- **UEDGE fluid model characteristics**
  - H-mode gradients;  $D=0.15 \text{ m}^2/\text{s}$ ,  $\chi_{e,i}=0.4 \text{ m}^2/\text{s}$
  - **Full drift physics model included**
- **General characteristics in good agreement**
  - In/out radial shift in  $T_e$ , opposite direction for  $n_e$
  - Partially attached ISP / well attached OSP
  - Target density peak inboard of the ISP
- **Confirms strong role of  $E_\theta \times B$  and  $E_r \times B$  drifts in asymmetry formation throughout the divertor region**



T. Rognlien, PSI2016  
A. Järvinen, EPS2016

# Modeling of DIII-D H-mode With $B \times \nabla B \downarrow$ and $\uparrow$ Using UEDGE Confirms Relative Roles of Poloidal and Radial $E \times B$ on Asymmetries

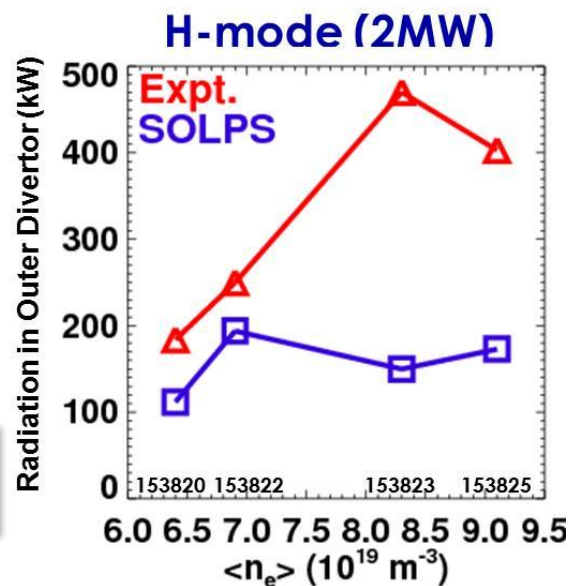
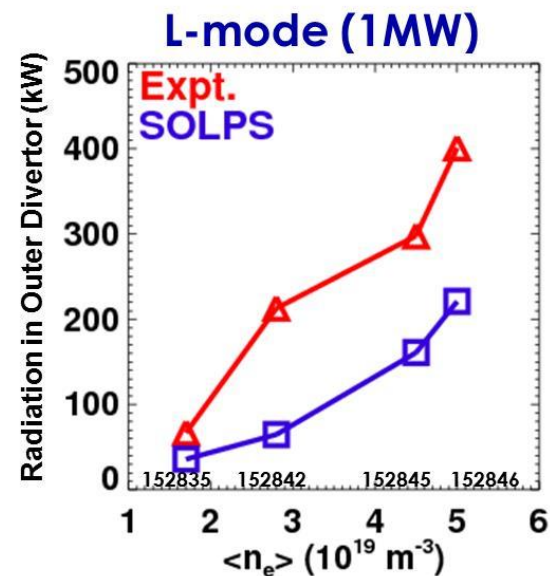
- H-mode gradients with drifts with  $B \times \nabla B \uparrow$  for the first time with UEDGE
- Again, general characteristics in good agreement
  - Improved symmetry in both  $T_e$  and  $n_e$
  - Stronger density peak outboard of the OSP
  - Displacement of peak conditions from target separatrix relative to  $B \times \nabla B \uparrow$  case confirms role of drifts in target asymmetries
- Underscore the importance of including  $E \times B$  effects in interpretive/predictive boundary modeling





# Matching Divertor Conditions and Eliminating Uncertain Molecular Physics Resolves Radiation “Shortfall”

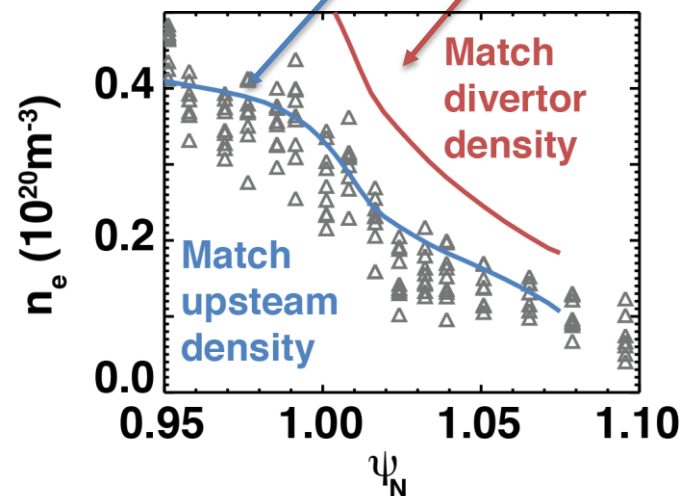
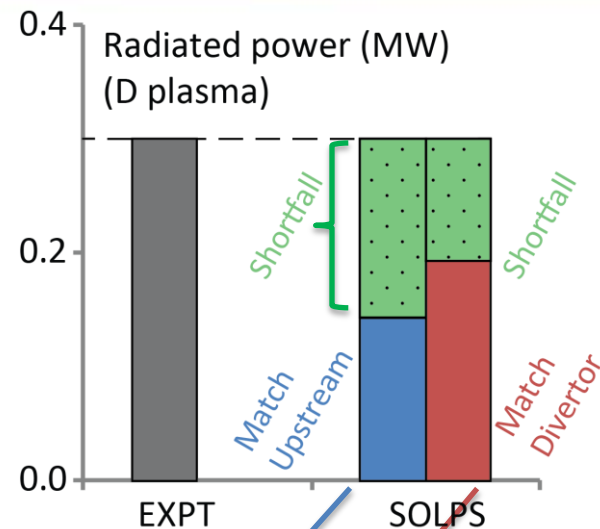
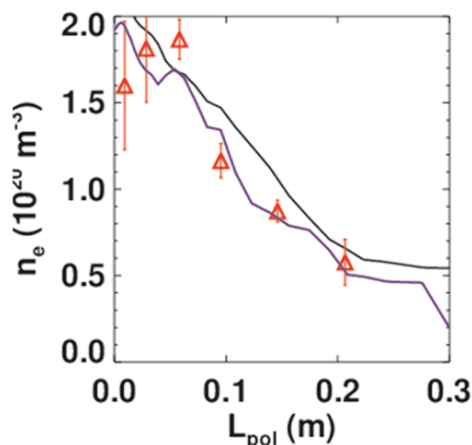
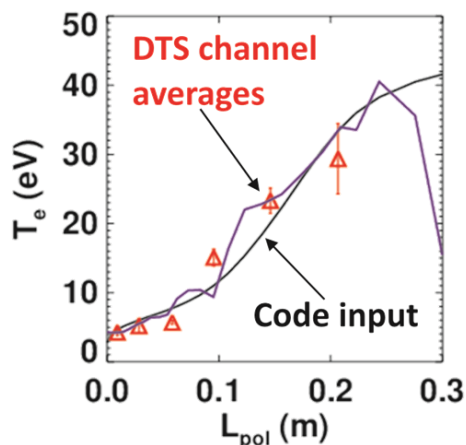
- Matching upstream conditions in fluid modeling leads to a shortfall in divertor radiated power relative to experiment
- Common result for DIII-D, JET, ASDEX
  - Multiple Braginskii fluid codes and wall materials
    - M. Groth, JNM2011 (UEDGE/DIII-D)
    - A. Järvinen, PPCF2016 (EDGE-2D+EIRENE/JET)
    - F. Reimold, PSI2016 (SOLPS/ASDEX)
    - J. Canik, PSI2016 (SOLPS/DIII-D)
- For DIII-D, both SOLPS and UEDGE modeling of D+C plasmas have shown this shortfall
  - L- and H-mode, all values of  $n/n_{GW}$



J. Canik, PSI2016  
J. Canik, APS2016

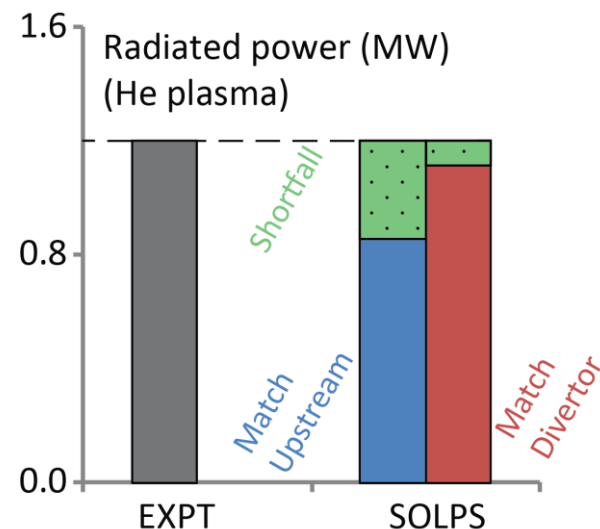
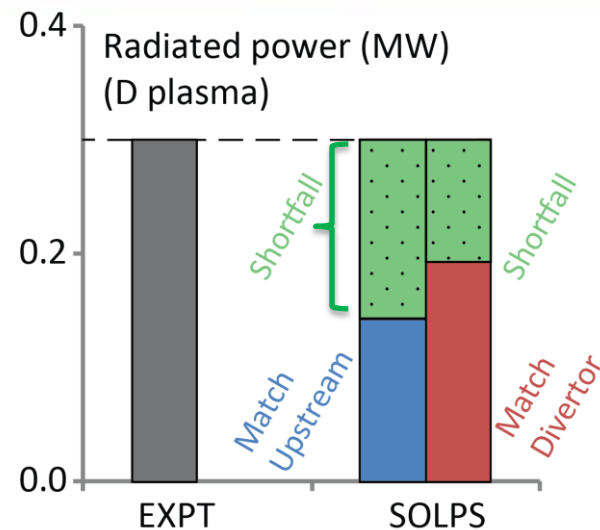
# Matching Divertor Conditions and Eliminating Uncertain Molecular Physics Resolves Radiation "Shortfall"

- However, the shortfall can be reduced using divertor plasma parameters from DTS (2D  $T_e$  and  $n_e$ ) as input
  - Allow upstream conditions to vary
- Suggests improvement needed in parallel physics model
  - Possible ion contribution to pressure/momentum



# Matching Divertor Conditions and Eliminating Uncertain Molecular Physics Resolves Radiation “Shortfall”

- **However, the shortfall can be reduced using divertor plasma parameters from DTS ( $2D T_e$  and  $n_e$ ) as input**
  - Allow upstream conditions to vary
- **Suggests improvement needed in parallel physics model**
  - Possible ion contribution to pressure/momentum
- **Additionally, the  $P_{rad}$  shortfall may be eliminated combining this technique with helium plasmas**
  - Removes uncertainty in hydrocarbon atomic/molecular physics
  - Consistent with result of M. Wischmeier, JNM2003 (B2.5-EIRENE/JET He plasma)



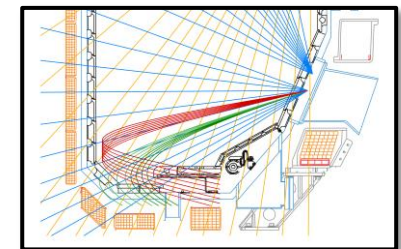
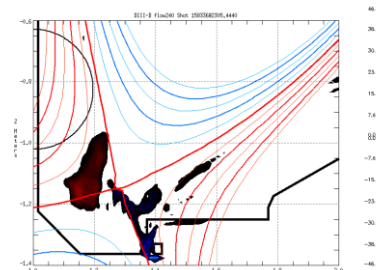
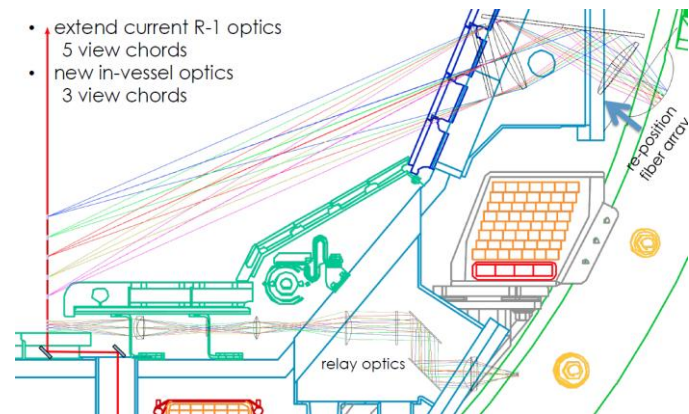
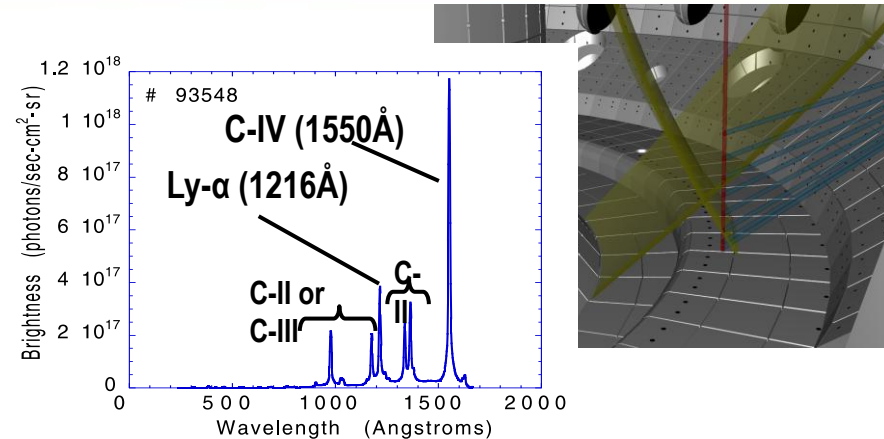
# Conclusions: Experiments With $B \times \nabla B$ $\downarrow$ and $\uparrow$ Provide Direct Evidence that Poloidal and Radial $E \times B$ Drifts Strongly Contribute to Target Asymmetries

- **Measured 2D divertor plasma parameters are directly interpreted to deduce poloidal and radial components of electric field, potential, and particle fluxes**
- **State-of-the-art fluid modeling in H-mode with a full drift model confirms major plasma characteristics**
  - Implications for heat flux control near a partial detachment operating point
- **A persistent/universal shortfall of radiation found with 2D edge fluid modeling of multiple machines and wall materials is improved using divertor conditions as input**
  - Modeling of He discharges suggests a combination of molecular physics and parallel transport are the cause
- **Comprehensive studies with extensive diagnosis provide valuable physics insight**
  - Demonstrates value of systematic parameter scans, necessity of physics inclusion in modeling



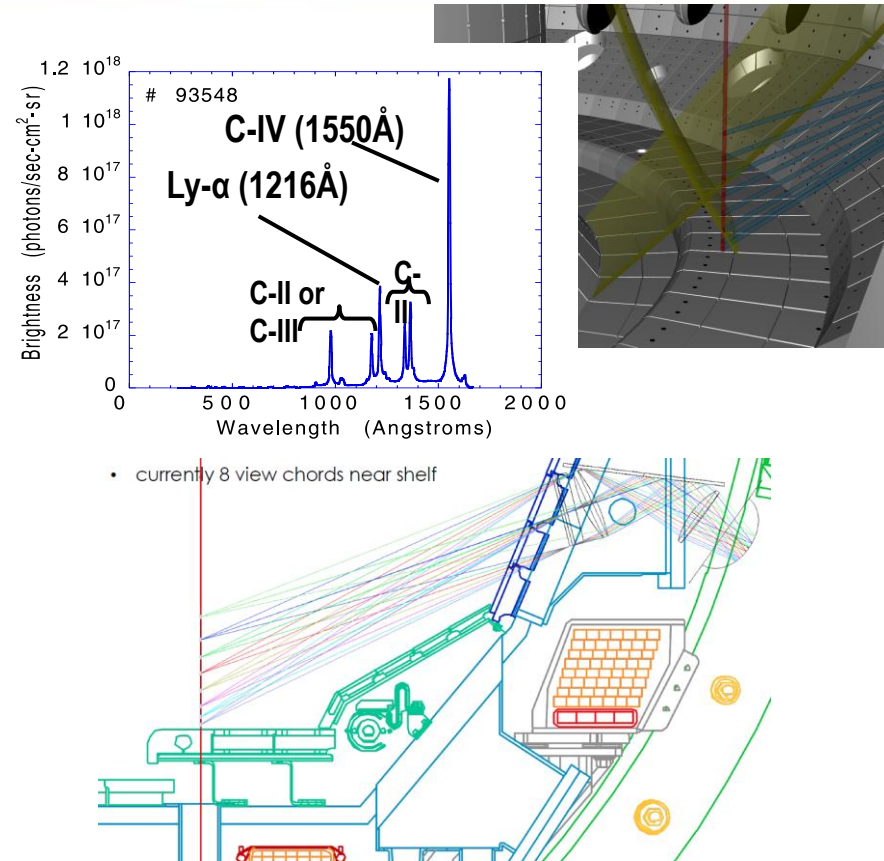
# Future Plans in Divertor Science on DIII-D

- **Addition of divertor EUV/VUV SPRED for fuel and impurity concentrations**
  - Direct measurement of radiative losses, and component concentrations
  - View coincident with DTS/spectroscopy
- **Divertor Thomson upgrades in progress**
  - Redirection of beam and collection optics to measure in high triangularity
  - Measurement frequency doubled to 100 Hz (2<sup>nd</sup> laser)
- **Flow interferometry in regular use**
  - CII/CIII/Hell parallel flow field
  - Improved calibration method implemented
- **Planned upgrade for divertor bolometry**
  - Addition of two high resolution fans in the lower divertor



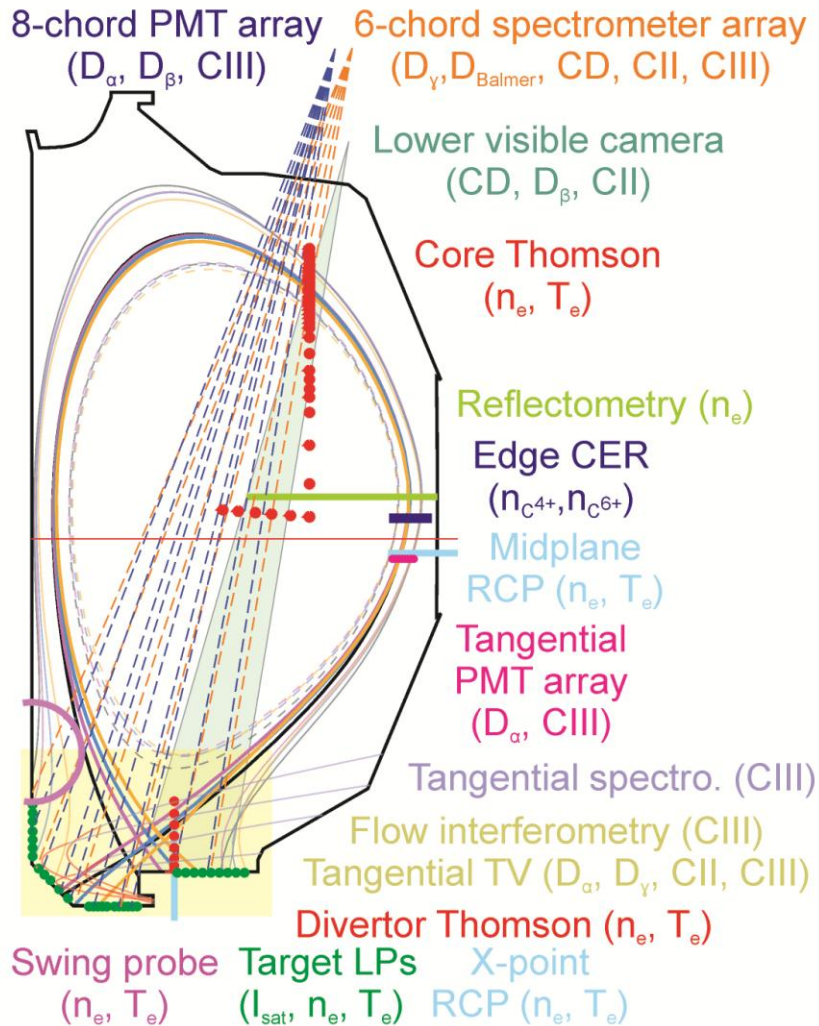
# Future Plans in Divertor Science on DIII-D

- **Addition of divertor EUV/VUV SPRED for fuel and impurity concentrations**
  - Direct measurement of radiative losses, and component concentrations
  - View coincident with DTS/spectroscopy
- **Divertor Thomson upgrades in progress**
  - Redirection of beam and collection optics to measure in high triangularity
  - Measurement frequency doubled to 100 Hz (2<sup>nd</sup> laser)
- **Flow interferometry in regular use**
  - CII/CIII/Hell parallel flow field
  - Improved calibration method implemented
- **Planned upgrade for divertor bolometry**
  - Addition of two high resolution fans in the lower divertor



# Backup slides

# DIII-D includes extensive lower divertor/boundary diagnostic coverage valuable for study of drift impact in attached and detached plasmas

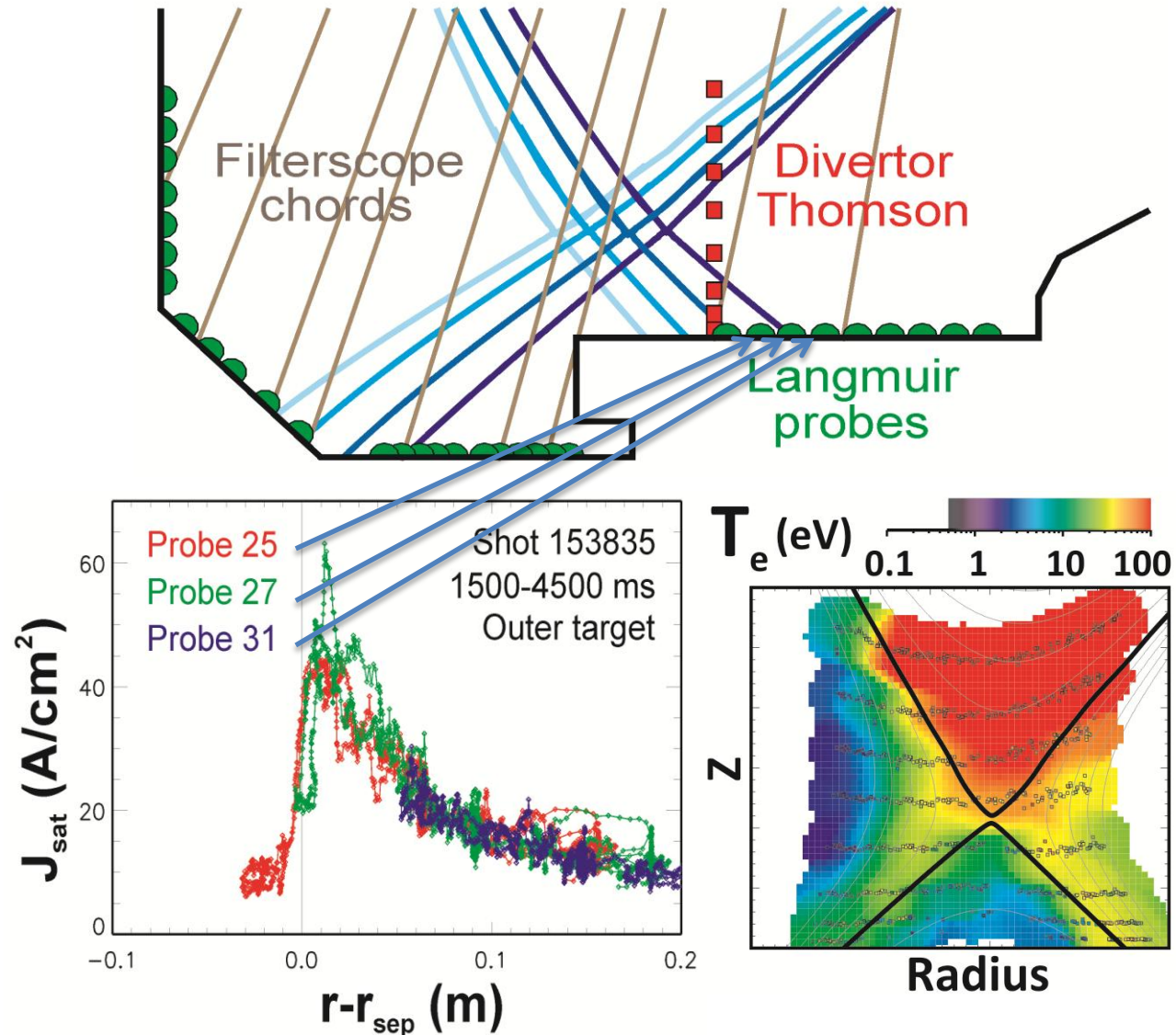


- **Improved 2D profiles of  $T_e$ ,  $n_e$ , e-pressure from DTS**
- Upstream profiles from core Thomson scattering, reciprocating (RCP), charge-exchange (CER), reflectometry
- Target particle flux from Langmuir probe array (LP) and visible cameras (DiMES TV)
- Heat flux from IR TV (floor view, and **periscope IRTV with full poloidal view**)
- Line emission profiles from PMT and visible divertor spectrometer arrays, tangential-viewing cameras (1D and 2D)
- **Toroidal impurity flows measured with interferometric cameras and tangential-viewing spectroscopy (1D and 2D)**
- Bolometer total radiation
- Neutral pressure measured with ASDEX ionization gauges in divertor and outer midplane



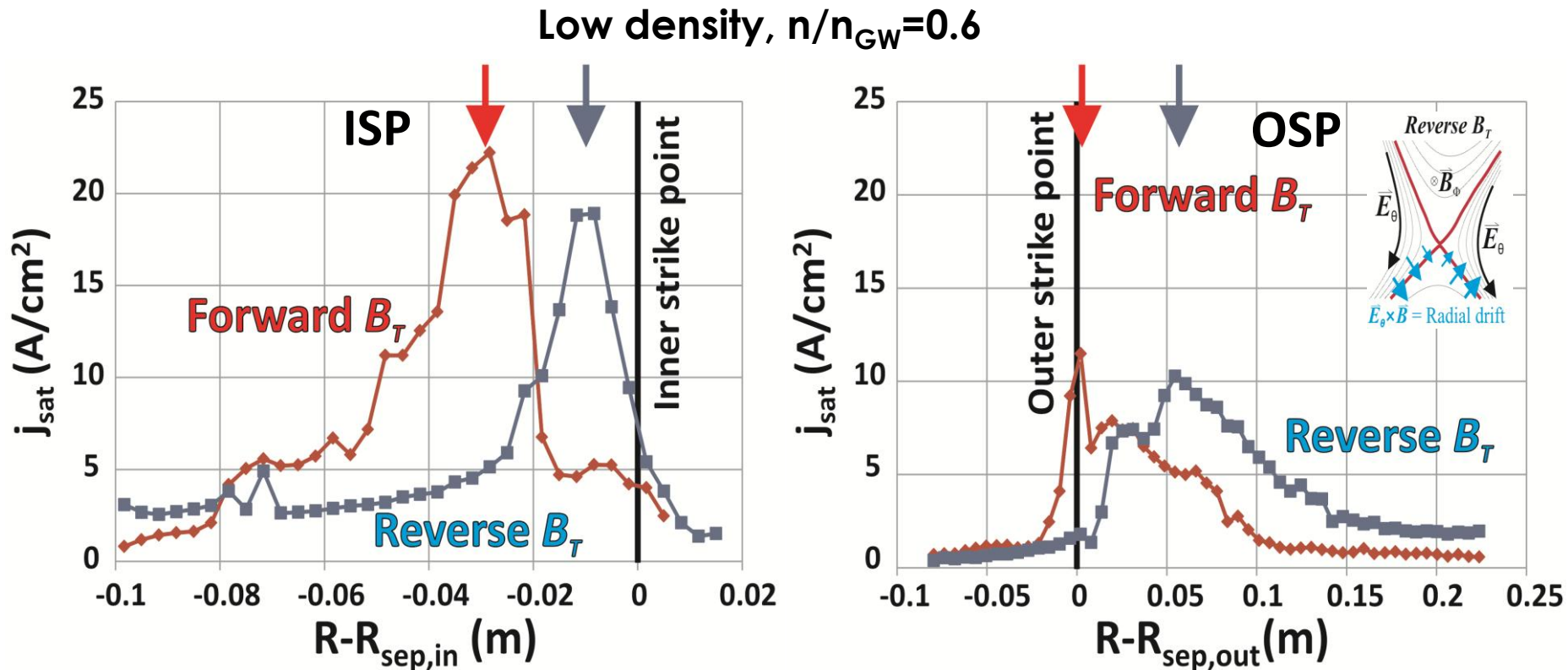
# Strike Point Sweeping With Constant Divertor Conditions is Used to Extend 1D Measurements To 2D

- DIII-D employs an open lower divertor, graphite first-wall tiles, and frequent conditioning
- Measurement of continuity in divertor conditions verified with mapped data from
  - Langmuir probes
  - Multichannel spectroscopy
  - Heat flux profiles
- Each step in the sweep used to reconstruct a 2D DTS profile



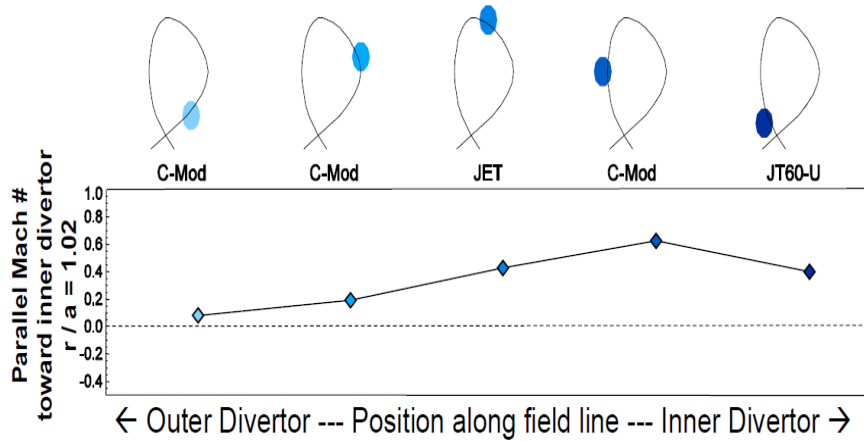
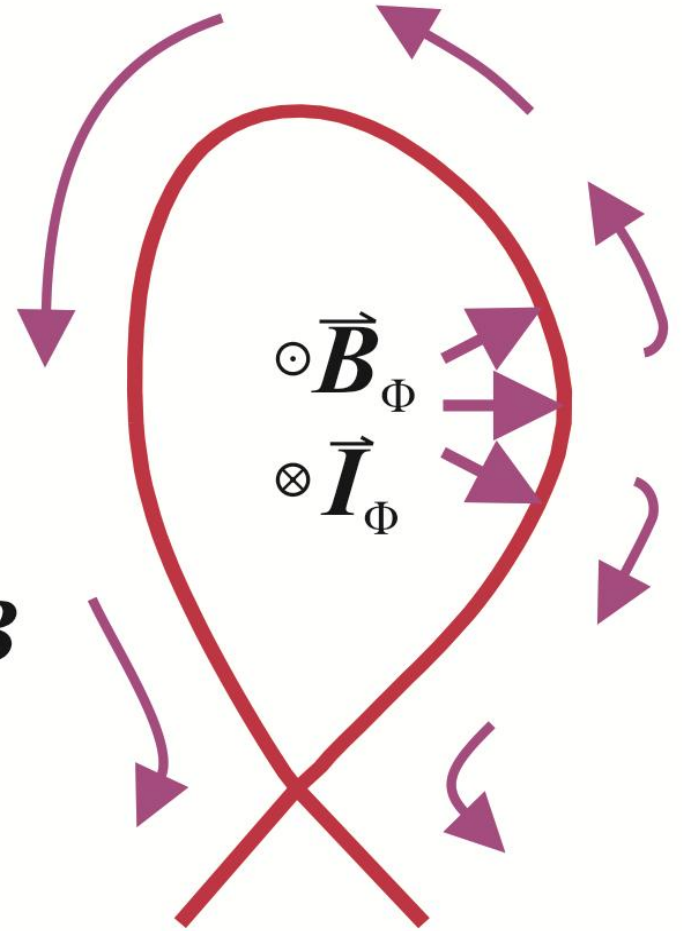
# Langmuir Probes Demonstrate Shifts of $j_{\text{sat}}$ and Plasma Potential as the B Field Reverses which Reduce as Density Increases

- $j_{\text{sat}}$  profiles shifted inward in forward  $B_T$  relative to reverse consistent with radial  $E \times B$  drift direction
- Smallest shift when poloidal temperature gradient is the least ( $E_\theta \propto dT/ds$ )
  - Simultaneous drop in plasma potential measured by the probes



# Strong ballooning-like parallel transport from the outboard midplane drives parallel flow around the SOL

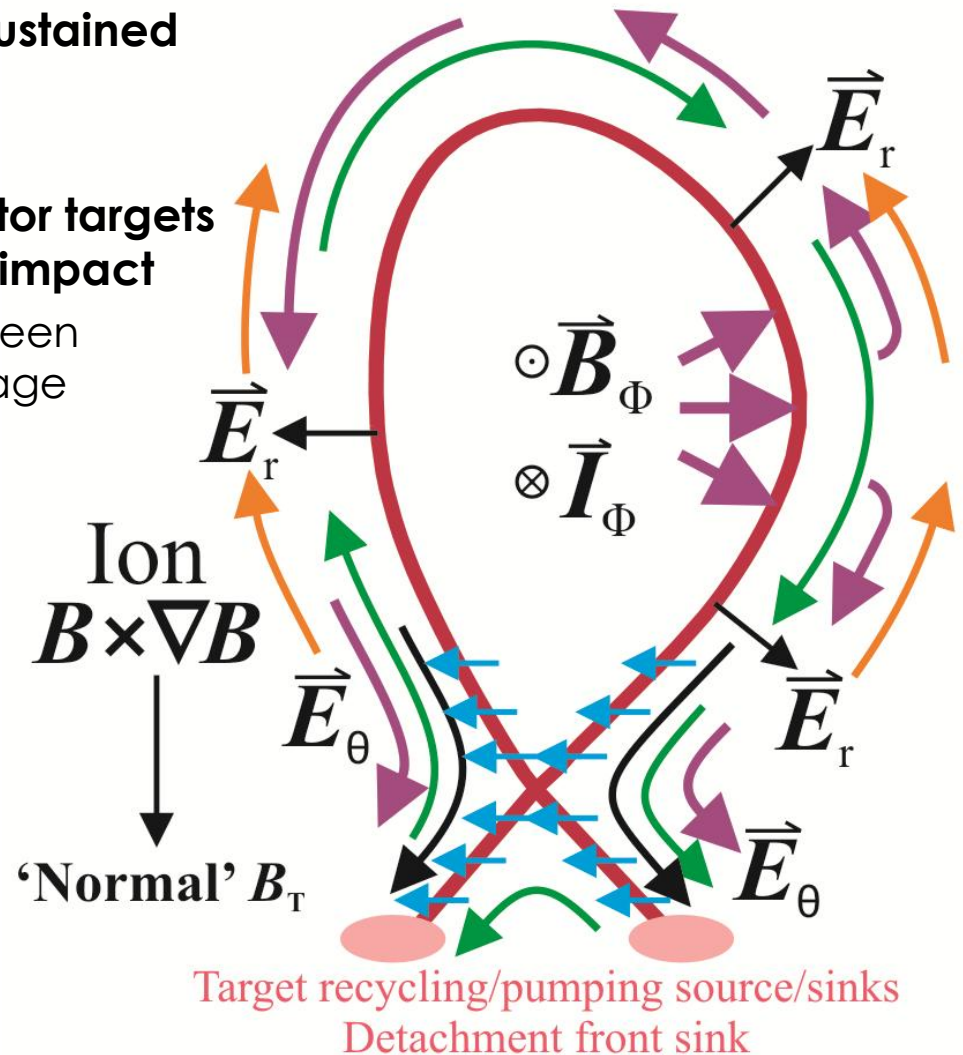
- Dominant cause of Mach~0.5 flow observed in plasma crown and HFS of C-Mod, JET, JT60-U and DIII-D
  - Smick, Nucl. Fusion 53 (2013) 023001.
  - Stangeby, J. Nucl. Mater. 415 (2011) S278.
- $\nabla \cdot \mathbf{V}_\theta + \nabla \cdot \mathbf{V}_r = 0$
- Stagnation point near outboard midplane
- Flow direction not dependent on B



Smick and LaBombard, PSI2010

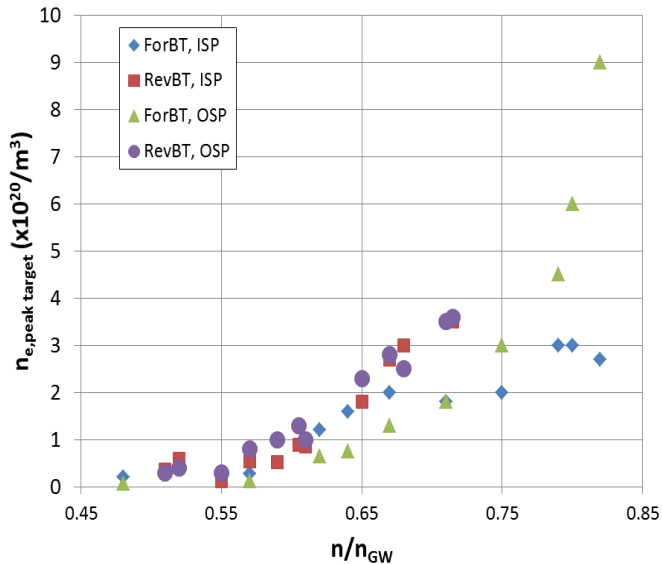
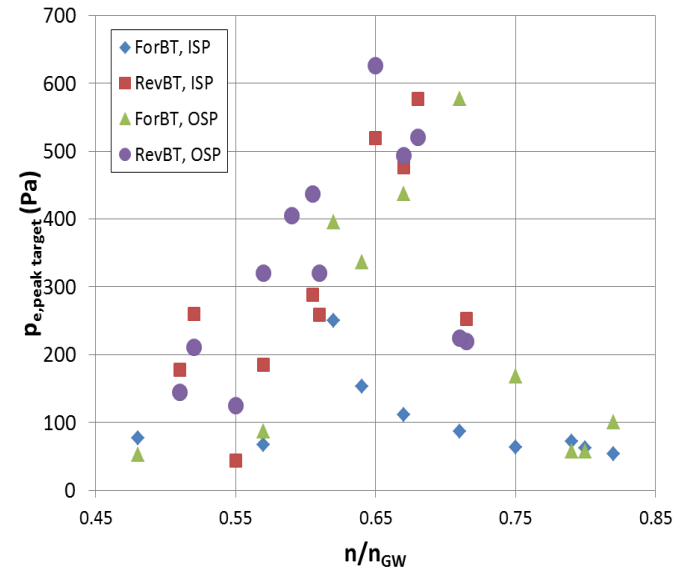
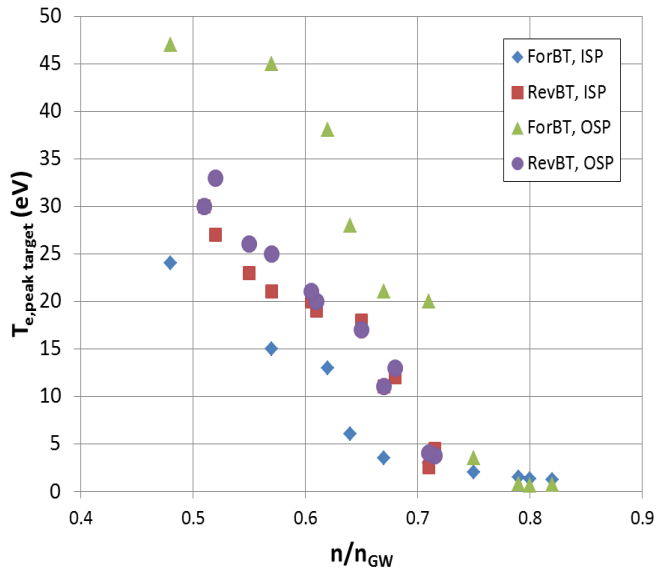
# Together, transport (parallel) and drift-driven (perpendicular) forces lead to a complex picture of particle/power flows around a tokamak

- Net poloidal rotation in the SOL gives rise to ion parallel Pfirsch-Schlüter flows sustained by up-down pressure asymmetry
- Ionization-driven flows at the divertor targets can additionally have large scale impact
  - Flow reversal and coupling between divertor legs due to neutral leakage
- Flows caused by  $\nabla B$  and centrifugal drifts, related to gradients of  $p/eBR$ , are relatively small
  - Pressure near equilibrium
  - Scale as  $1/\text{major radius}$  compared to  $E \times B$  which scales as  $1/\text{plasma scale length}$  ( $L_p \ll R$ )
  - Small variations in geometric volume factor  $R$





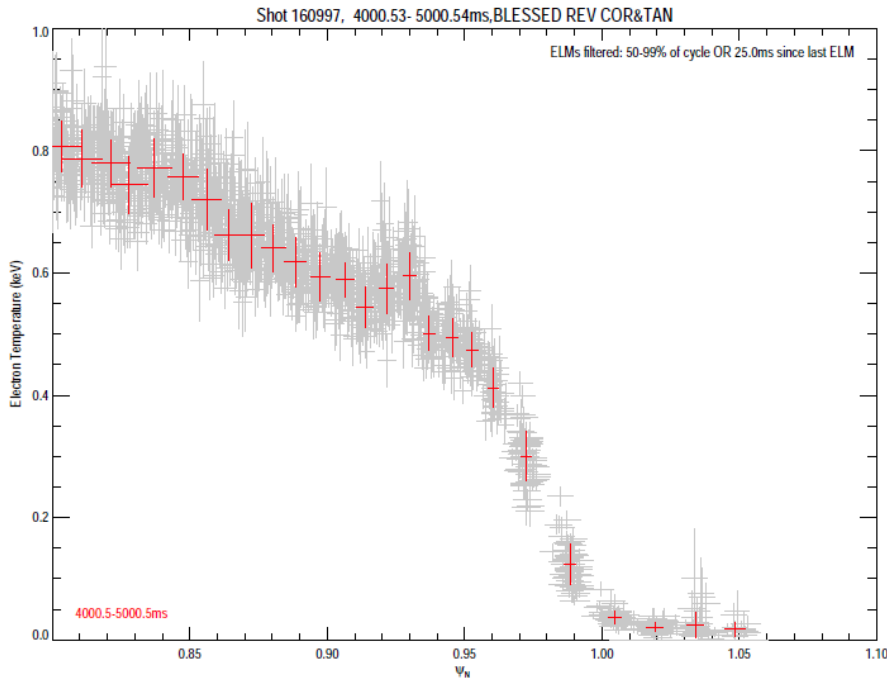
# Peak plasma conditions at the outer target, forward vs reverse $B_T$



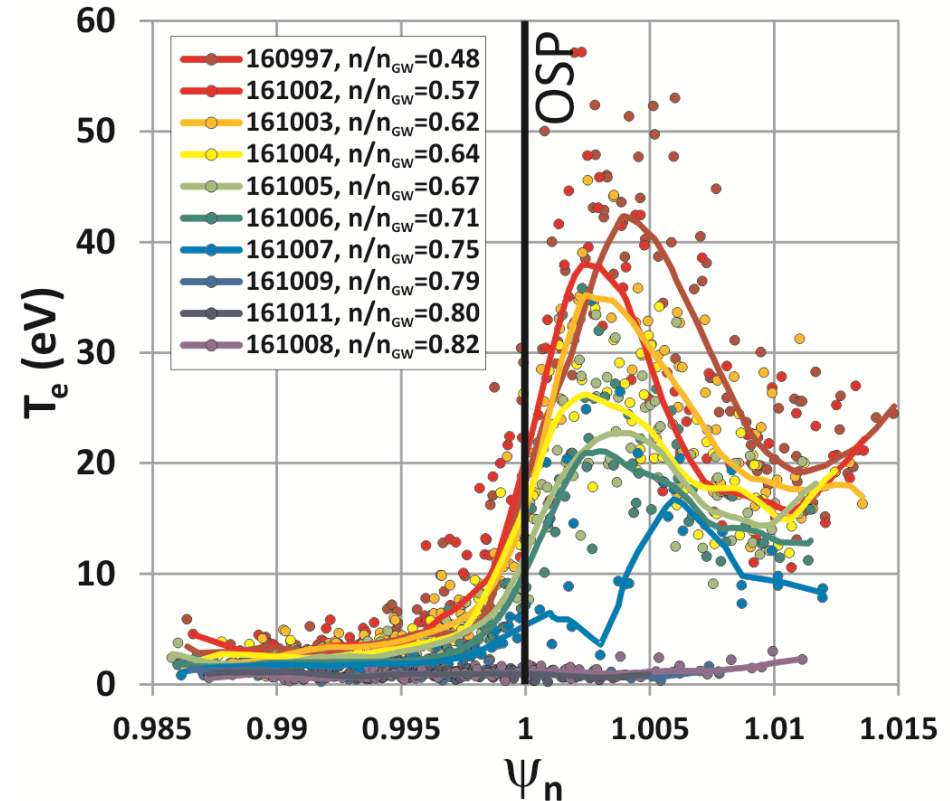
- $T_e$  cliff in fwd $B_T$  associated with  $\sim 10X$  drop in  $p_e$  ( $n/n_{GW}=0.72-0.78$ )
  - Largest fraction of drop in  $p_e$  occurs when  $T_e$  drops from 4 to 1 eV, not  $\sim 20$  to 4 eV
- OSP detached in rev $B_T$  does not have unusual drop in  $p_e$
- Symmetry in rev $B_T$  ISP/OSP peak values apparent compared to fwd $B_T$

# Raw Thomson data shows the influence of fluctuations captured by the system

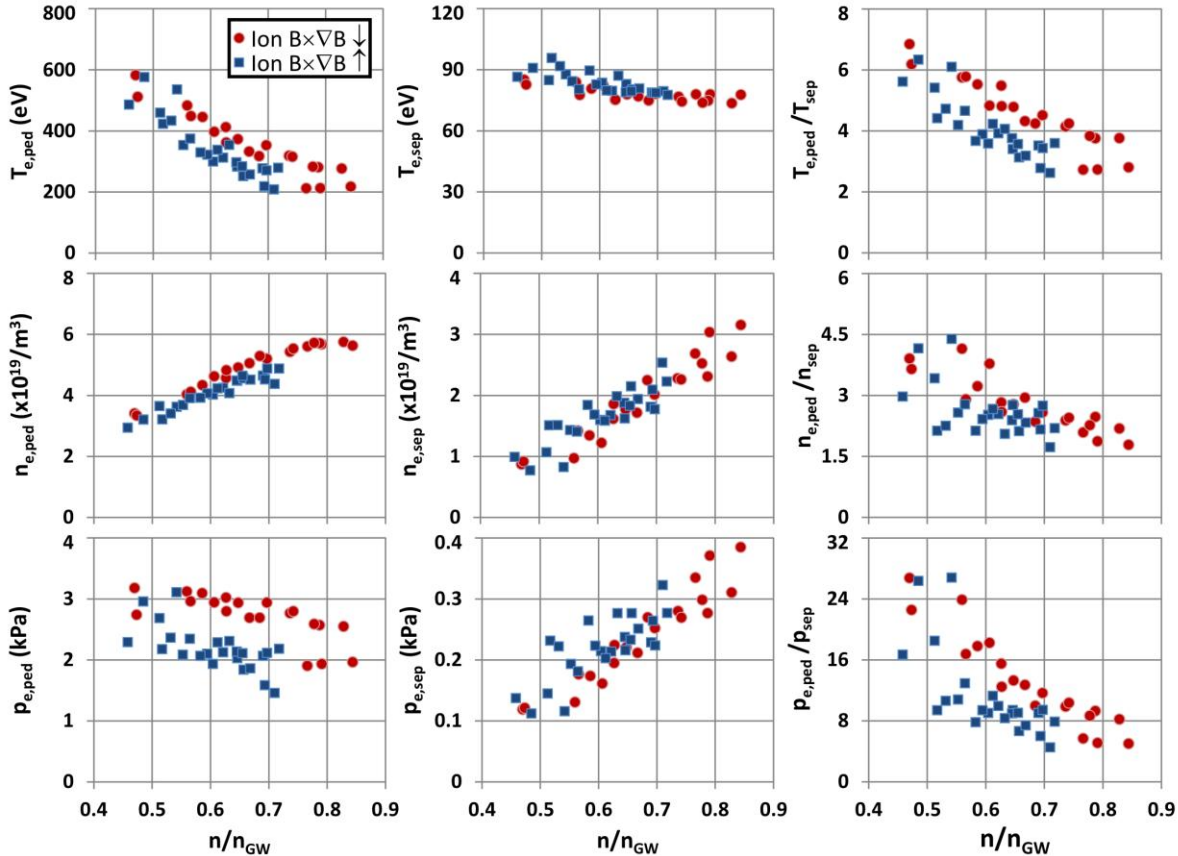
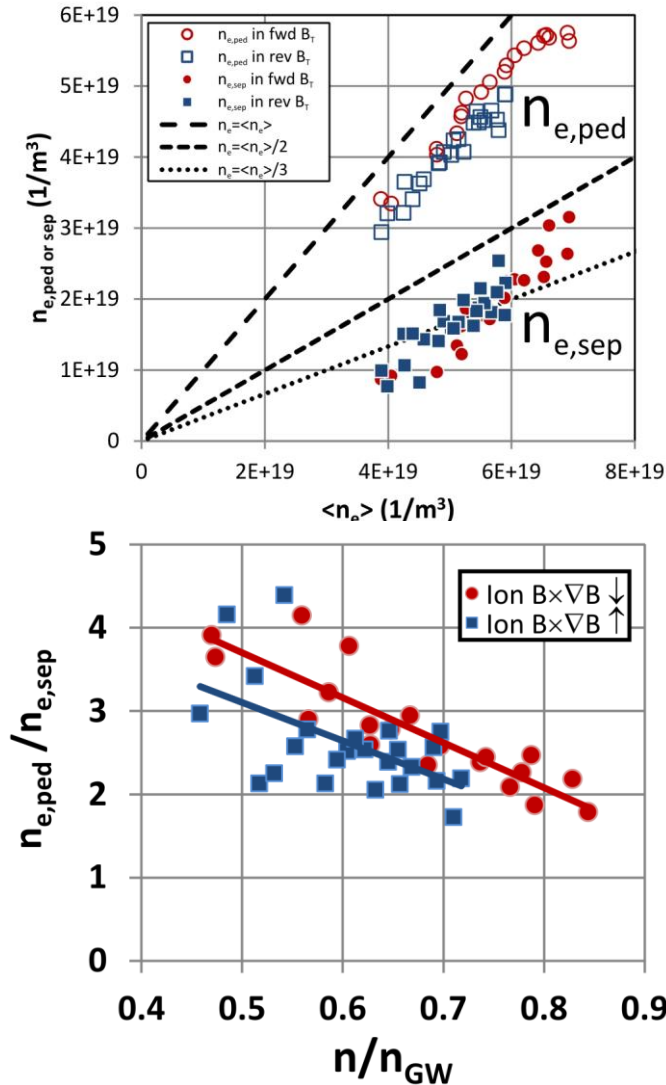
## Core/pedestal system



## Divertor system

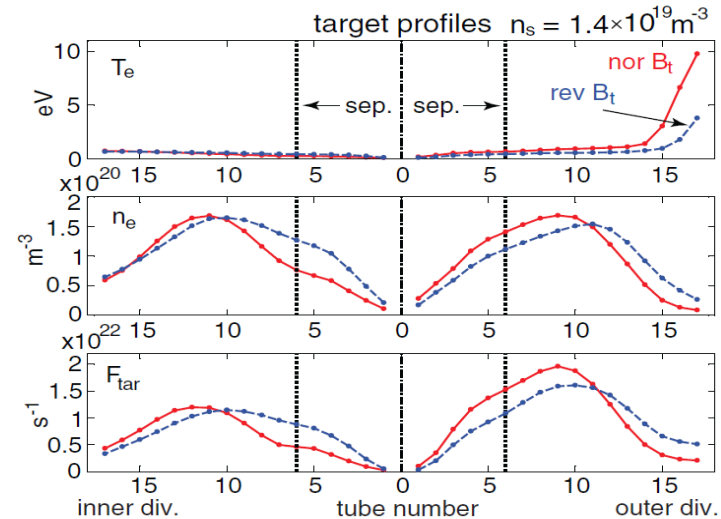
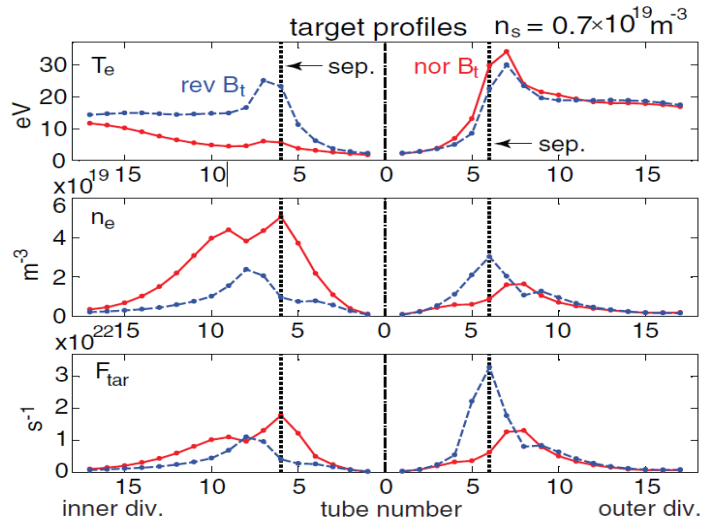
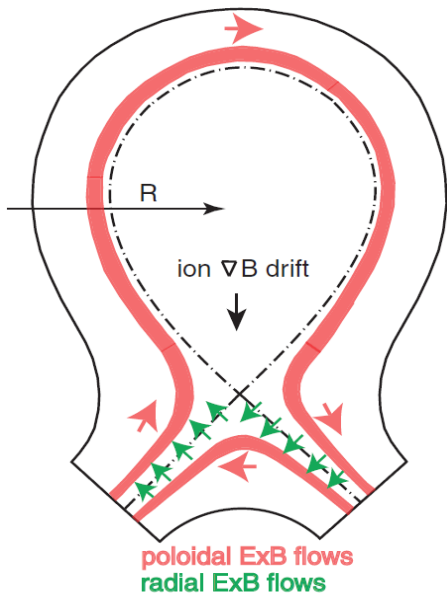


# Upstream/pedestal profiles demonstrate minor but systematic differences between fwd/rev Bt through the transition to detachment



# Recent modeling of JET strongly suggest $E_{\theta} \times B_{\phi}$ radial drift component is dominant prior to detachment onset

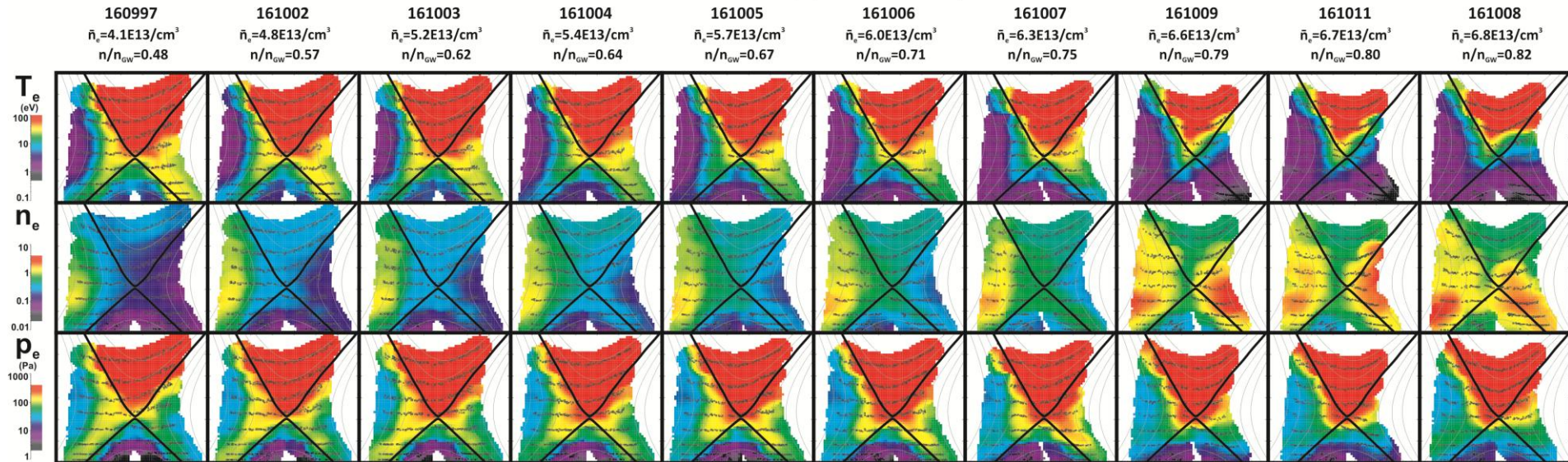
- Chankin/Groth JET EDGE2D results
- 2D edge fluid code of L-mode discharges with drifts included predict influence of  $B_t$  reversal on divertor and target asymmetries
- Analysis of convective fluxes caused by poloidal and radial  $E \times B$  drifts
- Crucial role of radial  $E \times B$  drift in influencing asymmetries
- Opposite to the result expected if poloidal  $E \times B$  drift was dominant in the divertor





# DTS: Forward $B_T$ (B x gradB down)

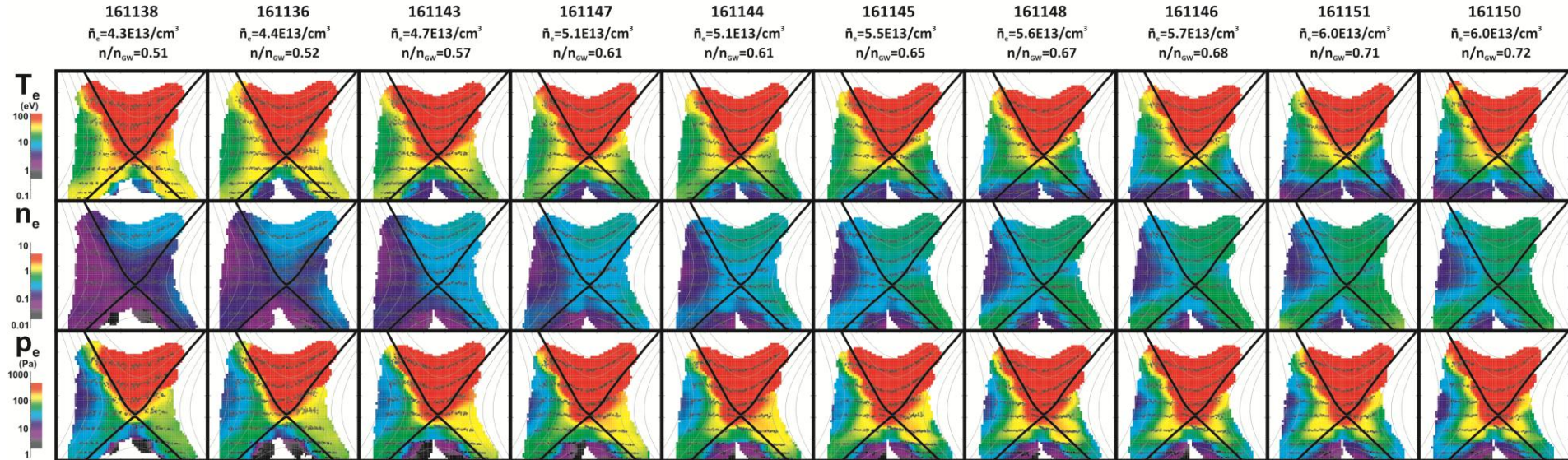
## Forward $B_T$ (ion $B \times \nabla B \downarrow$ )



- 10 step series,  $n/n_{GW}=0.48$  to  $0.82$
- Both targets attached to  $\sim 0.62$
- Inner target detaches smoothly from  $\sim 0.62$  to  $0.75$
- Outer target detaches suddenly from  $0.75$  to  $0.79$  (5% increase in  $n_{e,bar}$ ) – “Te cliff”
- Significant radial  $n_e$  gradient; highest at inboard from lowest  $n_e$  to  $n/n_{GW} \sim 0.75$
- Jump in  $p_e$  throughout divertor at high recycling onset ( $0.57$  to  $0.62$ ), slow decrease at inner target, jump down at outer target at point of detachment

# DTS: Reverse $B_T$ ( $B \times \text{grad}B$ up)

## Reverse $B_T$ (ion $B \times \nabla B \uparrow$ )

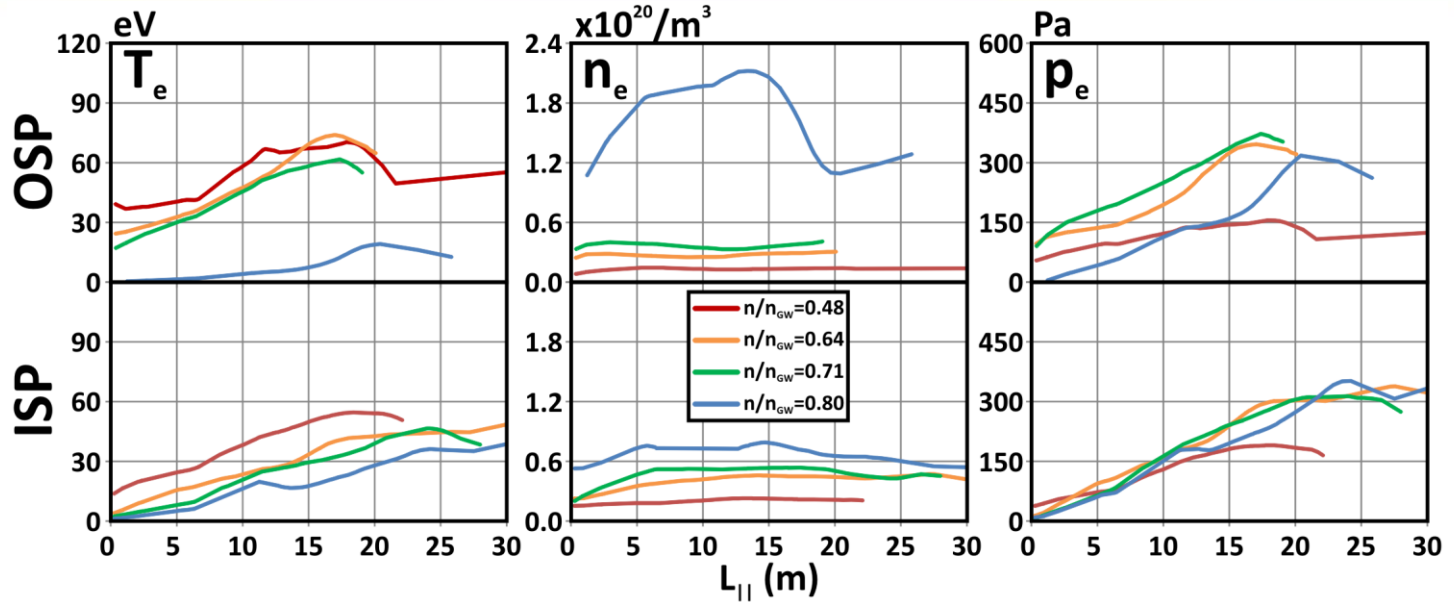


- **10 step series,  $n/n_{GW}=0.51$  to  $0.72$  (compared to  $0.48$  to  $0.82$  in fwd $B_T$ )**
  - Higher density attempts caused plasma to drop out of H-mode in rev $B_T$
- **Both targets attached to  $\sim 0.61$  (compared to  $\sim 0.62$  in fwd $B_T$ )**
- **Both targets detach together starting near  $\sim 0.65-0.67$  ( $\sim$ same as inner target in fwd $B_T$  case)**
- **Smaller  $n_e$  gradient, but upwards at higher major radius (i.e., wider low field side SOL)**
- **$p_e$  climbs then drops slowly at both targets**

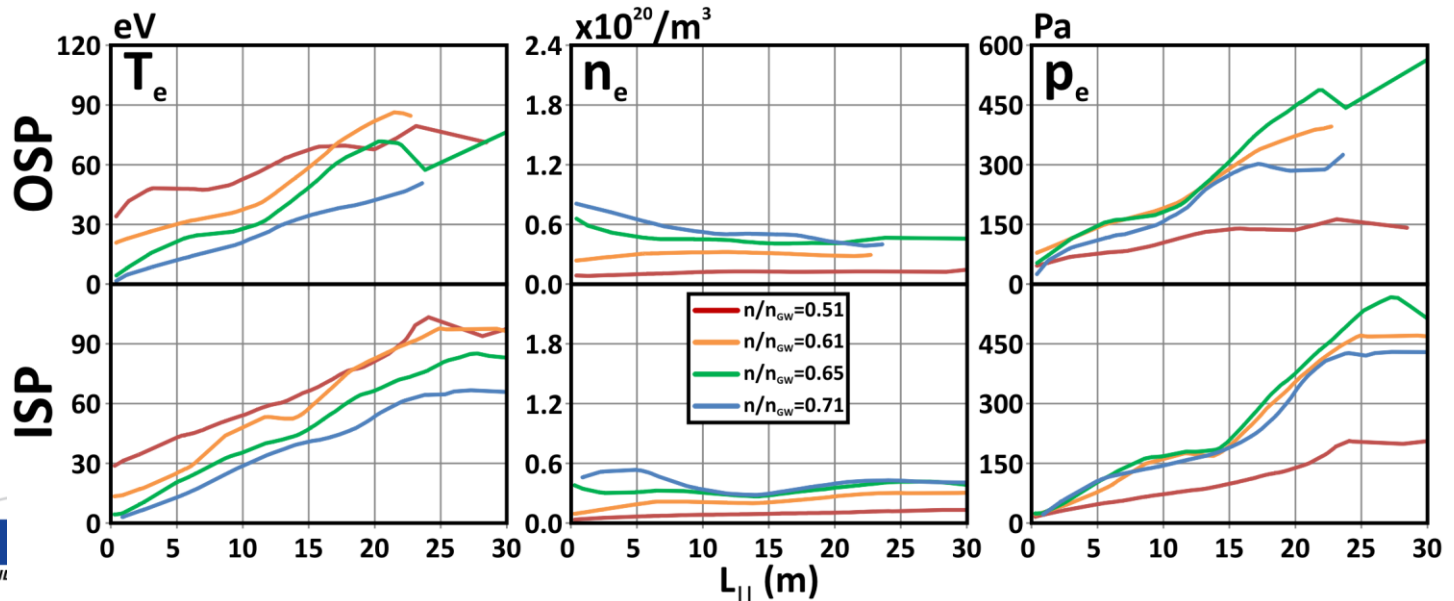


# DTS-measured parameters vs. $L_{||}$ demonstrate sudden transition to detachment along the entire OSP leg for fwd $B_T$

Forward  $B_T$



Reverse  $B_T$

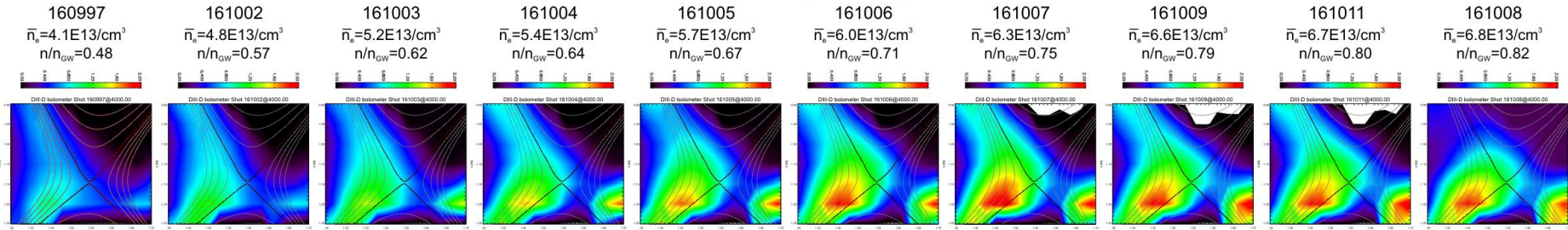


# Bolometry

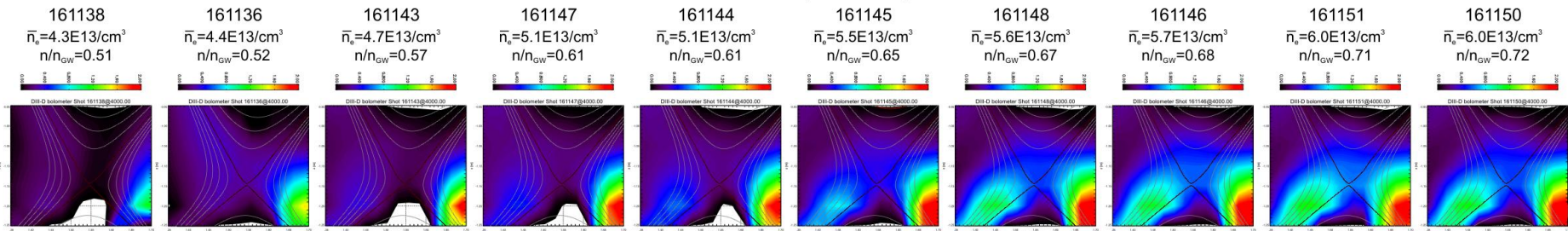
## DIII-D Bolometry

LSN 5.5 MW H-mode density scan,  $B_T = \pm 1.8T$ ,  $I_p = 0.9$  MA  
Data averaged from 3900-4100 ms in each shot

### Forward $B_T$ ( $B \times \nabla B \downarrow$ )



### Reverse $B_T$ ( $B \times \nabla B \uparrow$ )



- Same shots as in DTS series data (forward and reverse  $B_T$ )
- Inversion of data from 3900-4100 ms (ELM-averaged), both targets on the shelf